INTERNATIONAL ATOMIC ENERGY AGENCY
UNITED NATIONS EDUCATIONAL, SCIENTIFIC AND CULTURAL ORGANIZATION
INTERNATIONAL CENTRE FOR THEORETICAL PHYSICS
I.C.T.P., P.O. BOX 586, 34100 TRIESTE, ITALY, CABLE: CENTRATOM TRIESTE

SMR/382- 33

WORKSHOP ON SPACE PHYSICS:
"Materials in Micorgravity"
27 February - 17 March 1989

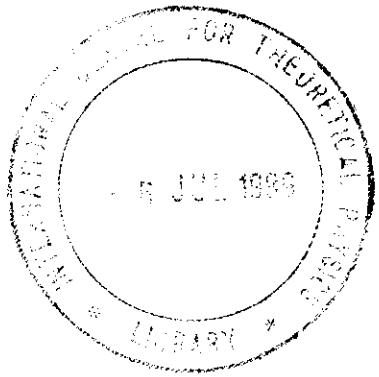

"Exploitation of Microgravity for Advanced Glasses"

C. BELOUET
Laboratoires de Marcoussis
Centre Recherche de la Compagnie Générale d'Electricité
Marcoussis, France

EXPLOITATION OF MICROGRAVITY FOR ADVANCED GLASSES

Christian BELOUET
LABORATOIRES DE MARCOUSSIS, Centre de Recherches de la
COMPAGNIE GENERALE D'ELECTRICITE
Route de Nozay - 91460 MARCOUSSIS (France)

This study, aimed at a prospectivce evaluation of glass processing in space, presents in succession the classical theory of glass transformation kinetics, the industrial perspectives in advanced glasses and the state of the art in Glass Processing in Space (GPS). It is shown that GPS definitely offers unique possibilities even though application areas cannot be clearly identified to-day. Finally, recommandations are put forward to exploit these new possibilities most efficiently.

I - INTRODUCTION

For a long time, glasses have been confined to domestic applications. Recently however, glasses have progressively entered most of the sectors of advanced technology. This situation naturally stems from the fact that i) glasses have properties which are superior in many instances to those of their crystalline counterparts, ii) glasses have an enormous compositional potential as compared with crystalline materials and iii) glasses can be made in almost any shape. A remarkable feature of the progress of glasses in advanced technology is that it is made by including borderline glass systems keen to devitrification in order to meet the demands of industry.

A number of authors have already suggested that the microgravity environment might procure new possibilities to prepare those glasses and to evaluate their intrinsic properties. This presentation is aimed at presenting the results of a one-year contract supported by ESA and dedicated to an assessment of the relevance of microgravity for the elaboration of advances glasses. It successively addresses the classical theory of glass transformation, the industrial perspectives in advanced glasses, the state of the art in glass processing in microgravity and the promising avenues for glass processing in space (GPS). Finally, recommendations are made for an efficient use of GPS.

II - NUCLEATION AND CRYSTALLIZATION IN GLASS FORMING MELTS

Glass formation occurs on cooling a liquid if crystal nucleation is avoided. Basic questions in glass technology are whether a material will form a glass when cooled from the liquid state and how fast a given material must be cooled so that detectable crystallization can be alleviated. Another question pertinent to this particular study is to evaluate the possible interplay of the gravity field in these processes.

In order to gain a better understanding of glass formation and stability, it is necessary to have a reliable and quantitative analysis of the transient nucleation of crystalline phases.

The classical theory of nucleation has been initially formulated by Volmer & Weber for vapour-to-solid transformations [1] and extended by Turnbull and Fischer [2] to liquid-to-solid transformations. The current state of the art of the theory of nucleation is given in the following.

II.1 - Classical nucleation theory, steady-state

II.1.1. Homogeneous case

Liquid-to-solid transformations are described with concepts based on the so-called classical nucleation theory. In this theory, it is assumed that clusters of molecules in a one component supercooled liquid, or formula units in a multicomponent supercooled liquid, arise in the original material in the configuration of the new phase. The free energy of formation of a cluster of n molecules, ΔG_n, is given by

$$\Delta G_n = n \Delta G' + A n \sigma \qquad (1)$$

where $\Delta G'$ is the difference in Gibbs free energy per molecule (or formula unit) between the new and the initial phases, A is the interface area of a cluster of n atoms, and σ is the interfacial free energy per unit area.

.../...

In the classical theory, it is postulated that $\Delta G'$ and σ have macroscopic values independent of n. Thus, it is not valid for very small clusters where an atomistic approach becomes necessary [3]. In the case of homogeneous nucleation spherical clusters are considered so that :

$$An = (36\pi)^{1/3} v^{2/3} n^{2/3} \quad (2)$$

where v is the molecular volume. This assumption leads to the classical formulation of ΔG_n

$$\Delta G_n = \frac{4}{3}\pi r^3 \Delta G_v + 4\pi r^2 \sigma \quad (3)$$

where ΔG_v is the difference in Gibbs free energy per unit volume.

Relations (1) and (2) do not account for cluster motion or stresses which may develop around the cluster as occurs in gas-to-liquid and solid-to-solid transformations respectively. The free energy of formation of a cluster is initially positive and exhibits a maximum ΔG_{n^*} as n increases, which forms an activation barrier against nucleation :

$$\Delta G_{n^*} = \frac{16\pi\sigma^3 V_m^2}{3\Delta G^2} \quad (3b)$$

where V_m is the molar volume of crystalline phase and $\Delta G = \Delta G_v$. V_m is the bulk free energy change per mole upon crystallization. At the maximum, a cluster of the new phase is in unstable equilibrium with the surrounding supercooled liquid. It is a critical cluster with a critical number of molecules n* and a critical radius r*. A smaller cluster-called an embryo - tends to decay spontaneously whereas a larger cluster-called a nucleus - tends to grow and thus is able to initiate crystallization.

.../...

In the classical theory of nucleation, clusters are assumed to arise by a series of reactions of the type given by Kelton et al. [4] :

$$E_{n-1} + E_1 \underset{k_n^-}{\overset{k_{n-1}^+}{\rightleftharpoons}} E_n \quad (4a)$$

$$E_n + E_1 \underset{k_{n+1}^-}{\overset{k_n^+}{\rightleftharpoons}} E_{n+1} \quad (4b)$$

Where n represents a cluster of n molecules and E_1 a single molecule, k_n^+ is the rate of addition of molecules to a cluster E_n and conversely, k_n^- is the rate of loss of molecules from E_n.

In their early development of nucleation theory, Volmer & Weber assumed that :

i) postcritical clusters grew rapidly (i.e., $N_n, t = 0$ for $n > n^*$) and,

ii) subcritical and critical clusters were at thermodynamical equilibrium (i.e., $N_n, t = N_n^e$ for $n \leqslant n^*$).

Using the formalism of Kelton et al. this led to a steady-state nucleation rate :

$$I = k_n^+ . N_n^e \quad (5)$$

with :

$$N_n^e = N^i \times \exp(-\Delta G_{n^*}/kT) \quad (6)$$

where N^i is the number of equivalent nucleation sites, i.e., the number of molecules - or formula units - in the initial phase. Relation (5) is currently given as :

$$I\ (L^{-3} . T^{-1}) = N \times \Upsilon \times n_s \exp(-\Delta G_{n^*}/kT) \quad (7)$$

.../...

where N is the number of molecules per unit volume, Υ is the impingement rate of molecules on sites available on the spherical surface of the cluster and n_s is the number of those sites.

The assumption of a discontinuity in the population of clusters at the critical size has been alleviated by formulating the kinetics as a steady-state process. Considering the transfer of molecules between embryos containing n and (n + 1) molecules according to reaction 4b, a steady-state distribution of clusters can be achieved such that the net forward rate :

$$I_{n,t} = k_n^+ \times N_{n,t} - k_{n+1}^- \times N_{n+1,t} \qquad (8)$$

can be constant, independent of time t and size n.

Then $$I_{n,t} = I^S = k_n^+ \times N_n^S - k_{n+1}^- \times N_{n+1}^S \qquad (9)$$

where I^S is the steady-state nucleation rate and N_n^S (N_{n+1}^S) is the number of clusters containing n (n + 1) molecules in the steady-sate.

Following this line it is straightforward to show from (8) that :

$$I_{n,t} = N_n^e \, O_n \Upsilon \exp(-\Delta gn/2\ kT) \left\{ \frac{N_{n,t}}{N_n^e} - \frac{N_{n+1,t}}{N_{n+1}^e} \right\} \qquad (10)$$

so that in the steady-state :

$$\frac{I^S}{N_n^e \, O_n \Upsilon \exp(-\Delta gn/2\ kT)} = \frac{N_n^S}{N_n^e} - \frac{N_{n+1}^S}{N_{n+1}^e} \qquad (11)$$

In relations (10) and (11), O_n is the number of sites on the nucleus surface where transformations from one phase to the other is possible, the term $\Upsilon \times \exp(-\Delta gn/2\ kT)$ is k_n^+ with Δgn being the free energy difference between clusters E_{n+1} and E_n.

.../...

Equation (11) can be written for each value of n restricted in the u, v intervals where u and v are integers such that $u < n^* < v$, with the following hypotheses on boundary conditions :

$$\begin{aligned} n \leqslant u,\ & N_n^S = N_n^e \\ n > v,\ & N_n^S = 0 \end{aligned} \qquad (12)$$

There follows :

$$I^S \times \sum_u^v \frac{1}{N_n^e \, O_n \Upsilon \exp(-\Delta gn/2\ kT)} = \frac{N_u^S}{N_u^e} - \frac{N_{v+1}^S}{N_{v+1}^e} = 1 \qquad (13)$$

Or :

$$I^S = \frac{1}{\sum_u^v N_n^e \, O_n \Upsilon \exp(-\Delta gn/2\ kT)} \qquad (14)$$

Complementary simplifying hypotheses, consistent with the above hypothesis, and based on the observation that the summation can be restricted to the values of n close to n* permit to establish the following relation for I^S :

$$I^S = N O_{n^*} \Upsilon \left(\frac{-\Delta G'}{6\ \pi\ kT\ n^*}\right)^{1/2} \exp\left(-\frac{\Delta Gn^*}{kT}\right) \qquad (15a)$$

comparing relations (7) and (15a) and noting that O_{n^*} may be identified with n_s it appears that the early evaluation of I^S must be corrected by the so-called Zeldovich factor Z,

$$Z = \left(\frac{-\Delta G'}{6\ \pi\ kT\ n^*}\right)^{1/2} \qquad (16)$$

which is typically found between 10^{-2} and 1.

.../...

A number of variants of relation (15b) have been proposed. They are based on possible substitutions e.g. :

- $\Upsilon = \exp - \Delta G_D/kT$, where ΔG_d is the activation energy for transport of a molecule (or formula unit) across the nucleus/matrix interface,
- $\nu \simeq kT/h$, where h is Planck's constant,
- $O_{n^*} = 4\ n^{*2/3}$ [4],
- $N^* \Delta G' = -2\ \Delta G_{n^*}$,
- etc...

Thus, the following complete formulas are also currently used :

$$I^S = N.\nu.(n^*_s/n^*)\left(\frac{\Delta G_{n^*}}{3\pi kT}\right)^{1/2} \exp -\left|\frac{(\Delta G_d + \Delta G_{n^*})}{kT}\right| \quad [5] \quad (15b)$$

where n^*_s can be identified with O_{n^*} or :

$$I_s = 2N.\nu.v^{1/3}\left(\frac{\sigma}{kT}\right)^{1/2} \exp -\left|\frac{(\Delta G_d + \Delta G_{n^*})}{kT}\right| \quad [6] \quad (15c)$$

where v is the volume of the molecular unit.

An accomodation numerical factor, $z < 1$, has also been introduced in the pre-exponential factor in order to take into account eventual hindrances accompanying the incorporation of building units in the nucleus [7].

Other modifications of relations (15a) to (15c) which may turn out to be hazardous are often used in practice in nucleation studies. Firstly, the pre-exponential factor is approximated within a few orders of magnitude to :

$$A = N \times \frac{kT}{h} \quad (17)$$

.../...

HETEROGENEOUS NUCLEATION

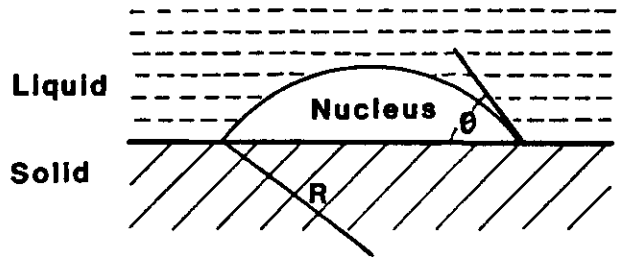

FIGURE 1

Heterogeneous nucleation : stability of an embryo of radius R on a substrate ; θ is the wetting angle.

where suscripts, c, ℓ and s refer to crystal, liquid and substrate and Θ is the contact angle.

The thermodynamic barrier ΔG^* to form crystal nuclei of radius r^* is reduced by a factor $f(\Theta)$,

$$f(\Theta) = \frac{1}{4} \cdot (2-3\cos\Theta + \cos^3\Theta) < 1 \qquad (24)$$

which is the ratio of the volume of the spherical segment to that of the corresponding entire sphere. Thus,

$$\Delta G^*_{het} = \Delta G^*_{hom} \times f(\Theta) < \Delta G^*_{hom} \qquad (25)$$

The reduction of the thermodynamic energy barrier which follows may be considerable as examplified in table 1 where $h = r(1 - \cos\Theta)$ is the height of the cap.

The nucleation rate I^s_{het} may still be written as I_{hom} with appropriate modifications :

$$I^s_{het} = N \cdot O_{n^*} \cdot \Upsilon \cdot Z \exp\left(-\frac{\Delta G_{n^*}}{kT}\right) \qquad (26)$$

here, N is the number of heterogeneous nucleation sites per unit volume - a number orders of magnitude smaller than the number of molecules per unit volume, O_{n^*} is reduced by a factor $f(\Theta)^{2/3}$ and ΔG_{n^*} by a factor $f(\Theta)$.

TABLE 1 :

f(Θ) for different h/r ratios, h being the height of the spherical cap

h/r	Θ°	(1 - cos Θ)/2	f (Θ)
2	180	1.00	1.00
1	90	0.50	0.50
0.5	60	0.25	0.156
0.25	41.4	0.125	0.043
0.125	28.9	0.011	0.062
0.062	20.3	0.031	0.003

.../...

thus, omitting O_{n^*}, Z and eventually z in relation (15). Secondly, the kinetic energy barrier ΔG_D is expressed in terms of an effective diffusion coefficient, D, in the liquid with :

$$D = D_o \exp(-\Delta G_D/kT) \qquad (18)$$

and

$$D_o = \frac{kT}{h}\lambda^2 \qquad (19)$$

where λ is the jump distance at the liquid/matrix interface, i.e., a quantity of the order of the molecule dimension. Thirdly, many authors relate D to the viscosity, η, of the liquid using the well-known Stokes-Einstein equation,

$$D = \frac{kT}{3\pi\lambda\eta} \qquad (20)$$

So that the steady-state nucleation rate may be written :

$$I^s = \left(\frac{A_c T}{\eta}\right) \times \exp\left(\frac{-\Delta G_{n^*}}{kT}\right) \qquad (21)$$

with :

$$A_c = \frac{Nk}{3\pi\lambda^3} \qquad (22)$$

using the relation $\Delta G_{n^*} = \frac{16\pi\sigma^3 V_m^2}{3} \times \frac{1}{\Delta G_v^2}$

II.1.2. Heterogeneous nucleation

Homogeneous nucleation is an intrinsic process which may be totally superseded by heterogeneous - or extrinsic - nucleation. Heterogeneous nucleation takes place on "substrate" particles which act as catalysts for the formation of stable nuclei - a spherical cap-shaped cluster of the type in fig. 1, growing on container walls or particles dispersed in the liquid, is eventually stabilized by surface forces σ at a critical radius r^* provided :

$$\sigma_{\ell,s} = \sigma_{c,s} + \sigma_{\ell,c} \times \cos\Theta \qquad (23)$$

.../...

Of main interest is the variation of the steady-state nucleation rate I^S as a function of absolute temperature in the cooling range $T < T_m$. Introducing the expression of Υ,

$$\Upsilon = \nu \exp -\Delta G_D/kT \qquad (27)$$

in relation (24) there comes :

$$I^S_{het,hom.} = N \cdot O_{n^*} \cdot \nu \cdot Z \exp - \Delta G_D/kT \times \exp - \Delta G_{n^*}/kT \qquad (28)$$

The dependence $I^S(T)$ is determined by the exponential terms. The first one accounts for the rate of addition of single molecules - or formula units -. It decreases monotonically with temperature as the mobility of molecules in the liquid is continuously reduced. The second exponential term which varies as $\exp - \left| \frac{1}{T.\ \Delta G_v^2} \right|$ decreases rapidly when T increases due to the corresponding increase of the thermodynamic barrier for the formation of a critical nucleus ; it vanishes with ΔG_v at $T = T_m$.

Therefore, the interplay of kinetical and thermodynamical processes gives the $I^S(T)$ curve a bell-shape.

II.2. Classical nucleation theory-transient state

Analytical treatments of transient nucleation are based on an approximation where n is continuous. Thus, using relation (10),

$$I_{n,t} = N_n^e \ k_n^+ \ \frac{N_{n,t}}{N_n^e} - \frac{N_{n+1,t}}{N_n^e}$$

and observing that $N_{n,t}$ changes according to :

$$\frac{\partial N_{n,t}}{\partial t} = I_{n-1,t} - I_{n,t} \qquad (29)$$

.../...

the Zeldovich-Frenkel equation [8,9] can readily be written as :

$$\frac{\partial N_{n,t}}{\partial t} = \frac{\partial}{\partial n} \left\{ N_n^e \ k_n^+ \ \frac{\partial}{\partial n} \left(\frac{N_{n,t}}{N_n^e} \right) \right\} \qquad (30)$$

Equations (6) and (28) can be combined to susbstitute N_n^e so that :

$$\frac{\partial N_{n,T}}{\partial t} = \frac{\partial}{\partial n} \left(k_n^+ \ \frac{\partial N_{n,t}}{\partial n} \right) + \frac{1}{kT} \ \frac{\partial}{\partial n} \left(k_n^+ \ N_{n,t} \ \frac{\partial \Delta Gn}{\partial n} \right) \qquad (31)$$

equation (31) and boundary conditions of the type in relation (12) are the basic ingredients for the calculation of $N_{n,t}$ anf $I_{n,t}$.

An exact analytical solution of equation (31) has not been obtained. Most authors have firstly considered that $I_{n^*,t}$ was representative of the nucleation rate experimentally observed and secondly introduced additional simplifying hypotheses to derive $I_{n^*,t}$ from equation (31).

The most thorough analytical treatments is due to Kashchiev [10] who obtained the following expression :

$$I_{n^*,t} = I^S \times \left| 1 + 2 \sum_{n=1}^{\infty} (-1)^m \exp (- m^2 \ t/\tau) \right| \qquad (32)$$

in which I^S is given by relation (15), n is an integer and τ is the nucleation time-lag,

$$\tau = \frac{- 24 \ kT \ n^*}{\pi^2 \ k_{n^*}^+ \ \Delta G'} = \frac{4}{\pi^3 \ k_{n^*}^+ \ Z^2} \qquad (33)$$

An alternative to the approximate analytical treatment above is the numerical treatment of basic equations (10) and (29), i.e.,

$$I_{n,t} = k_n^+ \cdot N_n^e \left[\frac{N_{n,t}}{N_n^e} - \frac{N_{n+1,t}}{N_{n+1}^e} \right] \qquad (10)$$

and

$$\frac{\partial N_{n,t}}{\partial t} = I_{n-1,t} - I_{n,t}$$

The first such treatment was made by Turnbull [2]. Recently, K.F. Kelton, A.L. Greer and C.V. Thompson made a detailed theoretical treatment of transient nucleation by numerical simulation [4].

They developed two methods in order to solve the system of coupled differential equations which describe nucleation in condensed phases (using equations (8) and (29)).

$$\frac{d N_{n,t}}{dt} = k_{n-1}^+ \times N_{n-1,t} - (k_n^- N_{n,t} + k_n^+ N_{n,t}) + k_{n+1}^- \times N_{n+1,t} \qquad (34)$$

In the first one, differential equation 34 is written in the matrix form, i.e. with the authors formulation :

$$\dot{N} = KN \qquad (35)$$

where,

$$N = \begin{bmatrix} N_{u,t} \\ N_{u+1,t} \\ \cdot \\ \cdot \\ \cdot \\ N_{v,t} \end{bmatrix}$$

.../...

and

$$K = \begin{bmatrix} -k_u^+ & k_{u+1}^- & 0 & 0 & \cdots & 0 \\ k_u^+ & -(k_{u+1}^- + k_{u+1}^+) & k_{u+2}^- & 0 & \cdots & 0 \\ 0 & 0 & -(k_{u+2}^- + k_{u+2}^-) & k_{u+3}^- & \cdots & 0 \\ \cdot & \cdot & \cdot & & & \cdot \\ \cdot & \cdot & \cdot & & & \cdot \\ \cdot & \cdot & \cdot & & & \cdot \\ \cdot & \cdot & \cdot & & & \cdot \\ 0 & 0 & \cdot & & & k_{v-1}^- - (k_v^- + k_v^+) \end{bmatrix} \qquad (36)$$

The hypotheses made by the authors fall into those of classical nucleation theory, e.g. the [u,v] range of n values is restricted to [9,3n*].

By diagonalizing matrix K,

$$A = B^{-1} K B \qquad (37)$$

they obtain the transformed equation

$$\dot{Y} = A.Y \qquad (38)$$

The solution is a vector with components

$$f_{n.t} = y_{n,o} \exp(\lambda_m t) \qquad (39)$$

where λ_m are the eigenvectors of the A matrix. Fixing the initial cluster distribution [N] and letting $b_{\ell m}$ be the element of the B matrix, the cluster concentration $N_{n,t}$ as a function of time and n is :

$$N_{n,t} = N_{1,0} \sum_{m=u}^{v} b_{nm} b_m^{-1} \exp(\lambda_m t) \qquad (40)$$

As postulated by the authors, this treatment can be applied to any isothermal, multistate rate problem with any initial population of states, where only transitions between neighbouring states are allowed.

.../...

The second method is a numerical technique which simulates directly the reactions involved in clusters formation and nucleation. The essence of the approach is to divide time into small intervals δt. In an interval, the probability of a cluster of size n gaining one molecule to form a cluster of size (n+1) is $\delta t \times k_n^+$. If the numbers of clusters of size n is $N_{n,t}$ at the start of the interval, then at the end of the interval, taking account of all transitions as in Eqs (4) the number is given by :

$$N_{n,t+\ t} = N_{n,t} + \delta t \left[- k_n^+ N_{n,t} - k_n^- N_{n,t} + k_{n-1}^+ N_{n-1,t} + k_{n+1}^- N_{n+1,t} \right] \tag{41}$$

this equation does not take into account the alteration in cluster population during the interval δt. Therefore, it is true only in the limit $\delta t \longrightarrow 0$ where it boils down to equation (34).

Actually, the appropriate value of δt to be used depends on the molecular rate of attachment, γ. In their calculations, K.F. Kelton et al. started with time intervals typically as small as $10^{-8}/\gamma$.

These authors have compared the cluster population at the critical size $N_{n^*,t}$ calculated by the exact and simulation analyses ; they found that the maximum deviation of the two estimates of $N_{n^*,t}$ at any instant was 0.2 %. This close agreement testifies to the validity of the numerical simulation algorithm which turns out to be computationally superior.

In the same study, they also compared the validity of analytical methods based on the continuum approximation. They found that Kashchiev's treatment closely approached the exact solution of the basic transient nucleation equation for sufficiently large n values.

The numerical treatments of K.F. Kelton et al. were emphasized in this presentation because they represented the most reliable and versatile treatments of transient nucleation. In their present formulation, they use the hypotheses of the classical theory of nucleation ; as such they cannot

.../...

describe nucleation processes with critical clusters containing a small number n^* of building units e.g. $n^* \sim 10$ or smaller. If such situations do occur, as it may be the case in heterogeneous nucleation, atomistic models of the type proposed by Walton for vapour-to-solid transformations should be used [3].

One essential feature of the analysis of Kelton et al. is that it may be extented to atomistic models.

At this point, the analytical formulation of $I_{n^*,t}$ by Kashchiev can be retained for further analyses of nucleation and growth kinetics. Then, the general expresion of $I_{n^*,t}$ is :

$$I_{n^*,t} = I_{(t)} = I^s \left[1 + 2\ C \sum_{m=1}^{\infty} (-1)^m \exp - (m^2 t/\tau) \right] \tag{42}$$

where C is a parameter which accounts for the initial cluster size distribution at t = 0 [10] ; C = 1 if the initial population of clusters is zero.

Knowing I(t), the number N(t) (L^{-3}) of nuclei formed at time t is :

$$N(t) = \int_o^t I\ (t')\ dt'$$

or

$$N(t) = I^s \left[t - (\pi^2/6) - 2\tau \sum_{n=1}^{\infty} (-1)^m/m^2 \exp (-m^2 t/\tau) \right] \tag{44}$$

expression (44) shows an effective time-lag $\tau^* = \frac{\pi\, 2\tau}{6}$, τ being given by relation (33).

Inspection of equations (44) and (15c) clearly indicates that N(t) can be substantially reduced by the elimination of very active crystallization sites, characterized by values of $f(\theta) \ll 1$ since i) τ varies as $\tau_h \cdot f(\theta)^{1/3}$ and ii) the thermodynamic barrier for nucleation varies as $\Delta G_{n^*} \times f(\theta)$ where τ_h and ΔG^*_n are the time-lag and the activation energy for homogeneous nucleation respectively.

.../...

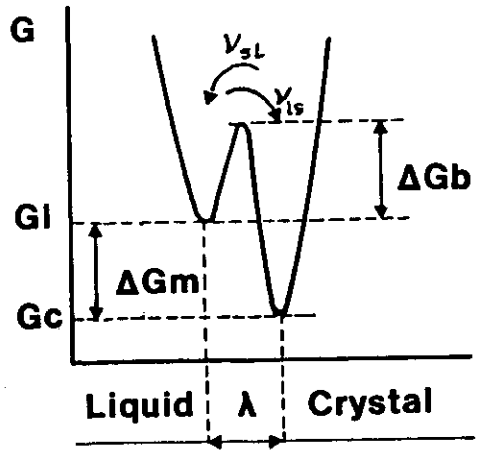

FIGURE 2

Surface-controlled growth mechanism

II.3 - Kinetics of overall crystallization

Stable nuclei formed either by homogeneous or heterogeneous nucleation grow at the expense of the adjacent fluid at a rate which depends on both the diffusion rate of the crystallizing species towards the solid-liquid interface and the rate of attachment of the species on the growth sites.

Thus, the crystallization rate of an undercooled liquid is specified by the rate of crystal nucleation, I, and by the speed, G, with which the crystal-liquid interface - or growth front - advances.

The growth speed, G, is controlled either by diffusion or by surface processes. Surface processes can be described by means of normal and lateral growth mechanisms [7]. For sake of simplicity, normal growth occurs on growth front rough on the atomic scale whereas lateral growth occurs on growth front smooth on the atomic scale. The former growth fronts provide a large relative fraction of attachment sites whereas the latter ones exhibits a small relative fraction located at i) the point of emergence of screw dislocations and ii) ledges of two-dimensional nuclei, e.g. [11,12]. Normal growth may be predicted for materials characterized by low entropies of fusion, namely $\Delta Sf < 2R$.

The general expression of the linear rate of growth for a surface limited process was given by D. Turnbull [13]. It was based on the model in fig. 2 where the crystal-liquid interface was specified by a double potential well extending over the jump distance λ .

Turnbull postulated that the net rate of growth, G, was proportional to the difference, $\nu^{\ell s} - \nu^{s\ell}$, where $\nu^{\ell s}$ and $\nu^{s\ell}$ were liquid (ℓ) - solid (s) transition rates, with :

$$\nu_{\ell s} = \nu \exp\left(-\frac{\Delta G_B}{RT}\right) \qquad (45a)$$

.../...

$$v_{s\ell} = \nu \exp - \left(\frac{\Delta G_B + \Delta G_m}{RT}\right) \qquad (45b)$$

In relations (45a, b), ν was the jump frequency factor ($\nu \sim \frac{kT}{h}$), ΔG_B was the barrier height at the growth front and ΔG_m was the molar Gibbs free energy difference accompanying crystallization. Thus, G was specified as :

$$G = f_{gs}\ \lambda \nu \exp\left(-\frac{\Delta G_B}{RT}\right)\left|1 - \exp\left(-\frac{\Delta G_m}{RT}\right)\right| \qquad (46)$$

where f_{gs} was the fraction of growth sites available and λ was the building unit jump distance.

Retaining the general assumption that ΔG_B may be identified with the activation energy for the diffusion of building units in the molten phase and using the Stokes-Einstein relation,

$$D = \frac{kT}{3\pi\lambda\eta} = \lambda^2 \nu \exp\left(-\frac{\Delta G_B}{RT}\right) \qquad (47)$$

expression (46) becomes :

$$G = k_h \cdot \beta_r \times \frac{kT}{3\pi\lambda^2\eta}\left|1 - \exp\left(-\frac{\Delta G_m}{RT}\right)\right| \qquad (48)$$

with $f_{gs} = k_h \times \beta_r$. In relation (48), $k_h \leq 1$ is a numerical factor accounting for possible hindrances during the incorporation of building units into the growth front and β_r, which depends on the growth mechanism, is the relative number of growth sites on the crystal surface.

In the case of normal growth, β_r is practically independent of ΔG_m and close to unity. Thus, at small ΔT (undercooling) values, using $\Delta G_m \cong \Delta S_f \times \Delta T$ where ΔS_f is the entropy of fusion, G appears to be linearly dependent on ΔT.

.../...

In the case of lateral growth, β_r is specified either by spiral growth - thus $\beta_r \simeq (\lambda/4\pi v_m \sigma)\ \Delta G_m$ and G varies as ΔT^2 at low ΔT values - or by the rate of formation of two-dimensional nuclei. In the latter case, $\beta_r \sim \exp - (W/RT)$ where the work of formation, W, of a two-dimensional nucleus is specified as,

$$W = \pi \sigma^2\ v_m\ \lambda / \Delta G_m \qquad (49)$$

G is then determined by an exponential factor of the form :

$$\exp\left(-\frac{A}{T.\Delta T}\right)$$

As this point, it is interesting to compare the general and separate dependences of the steady-state nucleation rate, I^s, and growth rate, G, on the reduced temperature, T_r, and undercooling, ΔT_r, which are defined as :

$$T_r = \frac{T}{T_m}, \qquad \Delta T_r = \frac{T - T_m}{T_m} \qquad (50)$$

where T_m and T are the crystallization point and actual absolute temperature respectively.

Using the approximated expressions,

$$\Delta H_f = \Delta S_f \cdot T_m \quad \text{and} \quad \Delta G_m = \Delta S_f \cdot \Delta T$$

with ΔH_f and ΔS_f being the molar heat and entropy of fusion respectively, it is straightforward to show that expressions (15) and (48) can be reduced, according to D. Turnbull's notation [14], to :

$$I^s = \frac{k_n}{\eta}\ e^{-b\,\alpha^3 \beta / T_r\ (\Delta T_r)^2} \qquad (51)$$

and

$$G = \frac{k_g}{\eta}\ f(\Delta T_r) \qquad (52)$$

.../...

where k_g and k_n are constants specified by nucleation and growth mechanisms, b is a constant determined by the shape of the nucleus, α and β are dimensionless parameters defined as :

$$\alpha = \frac{(N\ v_m^2)^{1/3}\ \sigma}{\Delta H_f}$$

$$\beta = \frac{\Delta S_f}{R}$$

where N is Avogadro's number.

A kinetic analysis of I^S (T_r, ΔT_r) and G (ΔT_r) based on simple nucleation theory and using expressions (51, 52) has been proposed by several authors. The major results of one such analysis due to D. Turnbull are summarized below.

The forms of the upper bound of I^S versus reduced undercooling, with different assigments to $\alpha\beta^{1/3}$, are plotted in fig. 3. In these calculations, the upper bound of I^S was obtained by setting η equal to 10^{-2} poise independent of temperature, k_n was given a typical value of 10^{30} dyn.cm [2] and b was assigned its value for a spherical nucleus, i.e. $16\pi/3$.

It follows from these curves that the upper bound of homogeneous nucleation rate I, though rising steeply with ΔT_r, is always negligible at small undercooling for practical values of $\alpha\beta^{1/3}$ currently $\gtrsim 1/2$ and goes through a maximum at $T_r = 1/3$ (α and β values reported in the literature lie between 1/4 to 1/2 and 1 to 10 respectively and $\alpha\beta^{1/3} \gtrsim 1/2$ is typical of metals and halides).

The $I(T_r)$ relation in fig. 4, for $\alpha\beta^{1/3} = 1/2$ indicates that corresponding liquids should resist homogeneous nucleation to a large undercooling. Indeed, the upper bound of I^S would be less than 1 $cm^{-3}.s^{-1}$ when $\Delta T_r < 0.18$.

.../...

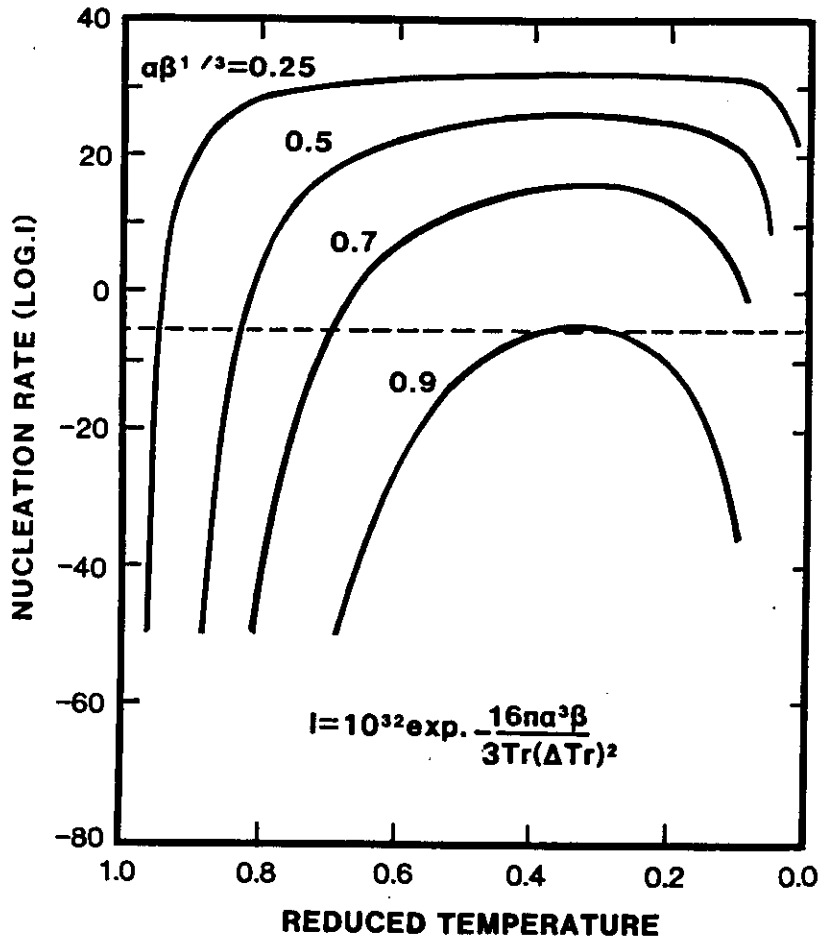

FIGURE 3

Exemple of calculated variation against temperature of the steady-state nucleation rate, I, (in $cm^{-3}.s^{-1}$, homogeneous case) in an undercooled liquid for various values of the parameter $\alpha\beta^{1/3}$.
The expression of I is given in the figure (after ref. 14)

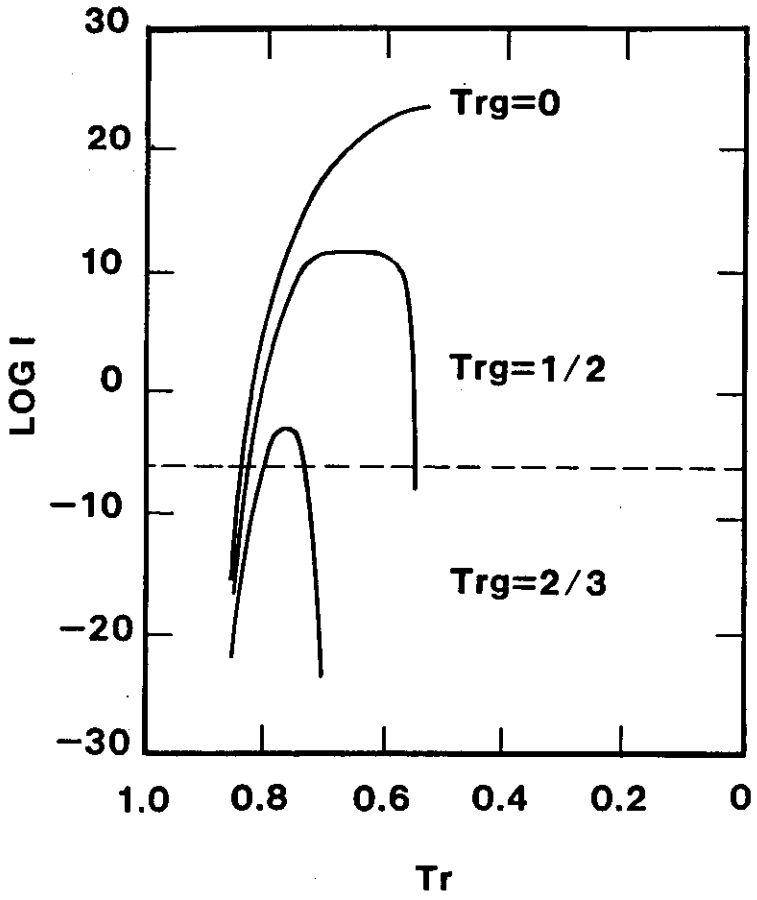

FIGURE 4

Example of calculated variation against temperature of the homogeneous nucleation rate I - $cm^{-3}.s^{-1}$ - (see fig. 3) for $\alpha\beta^{1/3} = 0.5$ and 3 trg values (after ref. 14)

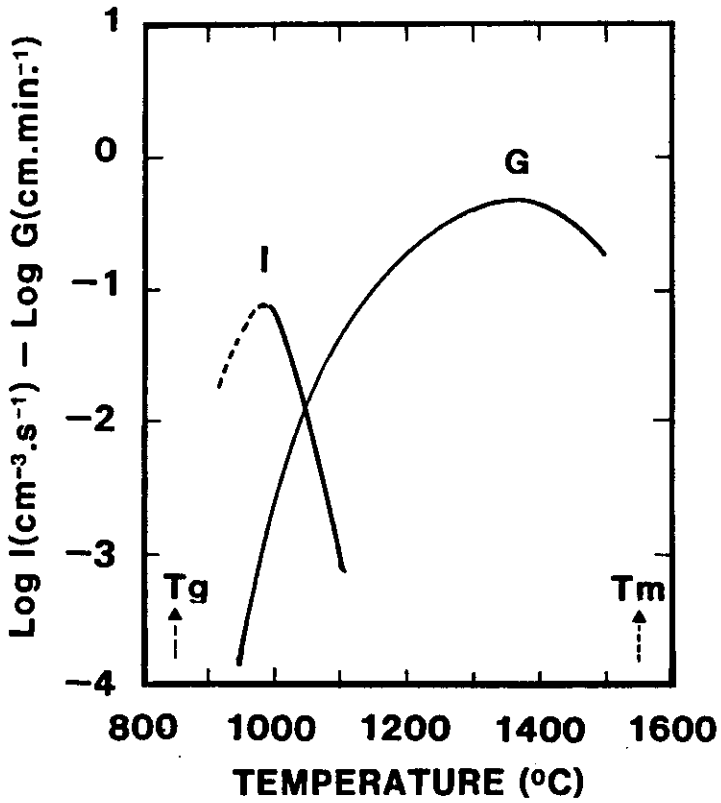

FIGURE 5

Measured nucleation rate, I, and growth rate, G, in anorthite system. A substantial overlap of the two processes is clearly visible (after ref. 16)

For the same $\alpha \beta^{1/3}$ value, Turnbull has derived the I^S (T_r) relation, for different assigments of $T_{rg} = T_g/T_m$ where T_g is the absolute temperature of glass transition, using the Vogel-Fulcher-Tammann (VFT) equation of viscosity [15],

$$\eta_{(poise)} = 10^{-3.3} \exp. \; 3.34/(T_r - T_g) \qquad (54)$$

Forms of I^S (T_r) relation are plotted in fig. 4. The effect of increasing T_{rg} is to lower, sharpen and shift to higher T_r, the peak in the Is (T_r) relation. For example, liquids specified by $T_g = 2/3\ T_m$ would exhibit a frequency of homogeneous nucleation relatively small and significant in a narrow range of undercooling only.

From these examples, it follows that the I^S (T_r) relationship has a bellshape and is characterized by a maximum whose position T_r (max) and magnitude I^S (max) vary considerably with the liquid properties. In all cases of practical relevance I^S for homogeneous nucleation is negligible at small undercooling.

This is in contrast with the G (T_r) relationship which gives bell-shaped curves with a maximum close to $T_r = 1$. Thus, depending on the system, crystallization and nucleation processes may either be practically separated or significantly overlap along the temperature scale. Fig. 5, after H. Yinnon and D.R. Uhlmann [16], is an experimental example for the anorthite system ($CaO - Al_2O_3 - 2\,SiO_2$) where a substantial overlap of the two processes is evidenced.

Fig. 6 is a general representation of $I^S(T)$, G(T) relations which shows the domains where nucleation and crystallization rates are significant. The critical region in the case of homogeneous nucleation is specified by the T_2, T_3 interval where both I^S and G are not negligible simultaneously.

If heterogeneous nucleation takes place this interval is shifted towards higher temperatures (T_r eventually reaches 1) and crystallization cannot generally be avoided.

The examples of SiO_2 and Al_2O_3 treated by D.C. Larsen [17] are of interest in this discussion.

.../...

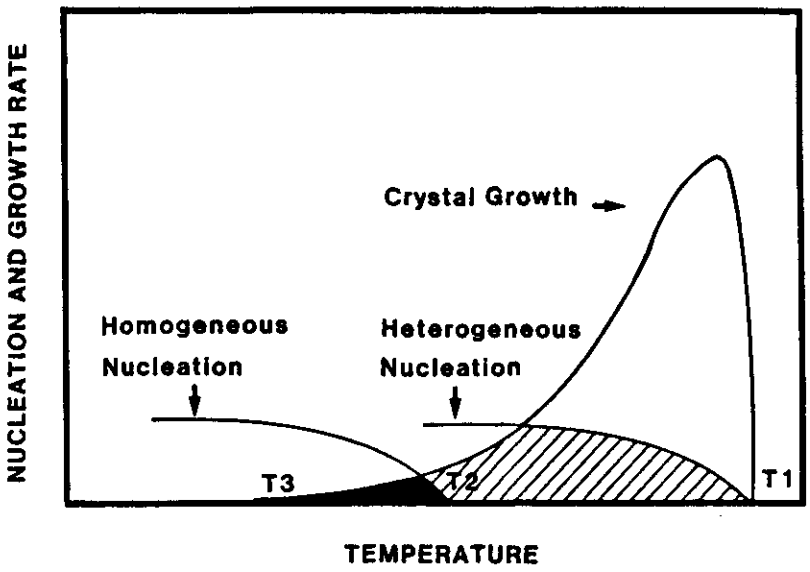

FIGURE 6

Nucleation rates and growth rates of a hypothetical system. T_m is the melting point

Materials parameters listed in tables 2.3 and equations 15, 48 were used to derive (homogeneous) nucleation and growth kinetics. The results obtained for silica are plotted in figs 7 to 9. It appears from this work that detectable nucleation does not occur upon cooling from the melt until 1700 K and that the growth rate, G SiO_2, peaks at an amazingly small value of 4 nm/min at a 50 K undercooling. Furthermore, no detectable crystallization can be obtained if the T_2, T_3 interval of overlap (1600-1700 K) is passed in typically less than 5.10^3s, i.e. at a cooling rate readily achievable in conventional processes.

The same analysis was applied to the Al_2O_3 system, which does not exhibit glass-forming tendencies by conventional processes on earth. If homogeneous nucleation and subsequent growth are considered as above, the region of overlap (1300-1625 K, fig. 10) should be passed rapidly. However, experience repeatedly shows that crystallization starts immediately upon cooling below the melting temperature. The reason for this may be accounted for by the occurrence of heterogeneous nucleation and the rapid growth rate of Al_2O_3, which peaks at around 10^9 nm/min (not accounting for the rate of dissipation of the heat of crystallization). The discrepancy between the predictions of homogeneous nucleation and experimental facts strongly suggest that an extrinsic property - heterogeneous nucleation - controls the glass-forming tendency of Al_2O_3 on earth. On the contrary, the example of SiO_2 is interesting in that it shows the relative insensitivity of this material, largely exploited in industry, to heterogeneous nucleation.

The steady-state $I(T_r)$ and $G(T_r)$ relations are most valuable to establish the capability of a substance to solidify in glass form. Equally important is the study of the time-dependent degree of crystallization, $x(t)$, of the liquid defined as

$$x(t) = V(t) / V_o \qquad (55)$$

where V is the volume crystallized at time t and V_o is the initial volume of the liquid.

.../...

TABLE 2

MATERIALS PARAMETERS FOR SiO_2

ΔH_f	=	2000 cal $mole^{-1}$
T_m	=	2000 K
ΔS_f	=	$\Delta H_f/T_m$ = 1 cal $mole^{-1}K^{-1}$
β	=	$\Delta S_f/R \sim .5$
λ	=	2.5 Å (~ 0-0 distance in SiO_4 tetrahedron)
β_r	=	1
V_m	=	27.6 cc $mole^{-1}$
α	=	2.5
n	=	$N/V_m = 2 \times 10^{22}$ molecules cc^{-1}
ΔT	=	$T_m - T$

TABLE 3

MATERIALS PARAMETERS FOR Al_2O_3

T_m	=	2300 K
λ	=	2.5 Å
β_r	=	1
ΔH_f	=	26,000 cal $mole^{-1}$
ΔS_f	=	11.3 cal $mole^{-1}K^{-1}$
β	=	5.65
α	=	2, 2.5, 3 (variable)

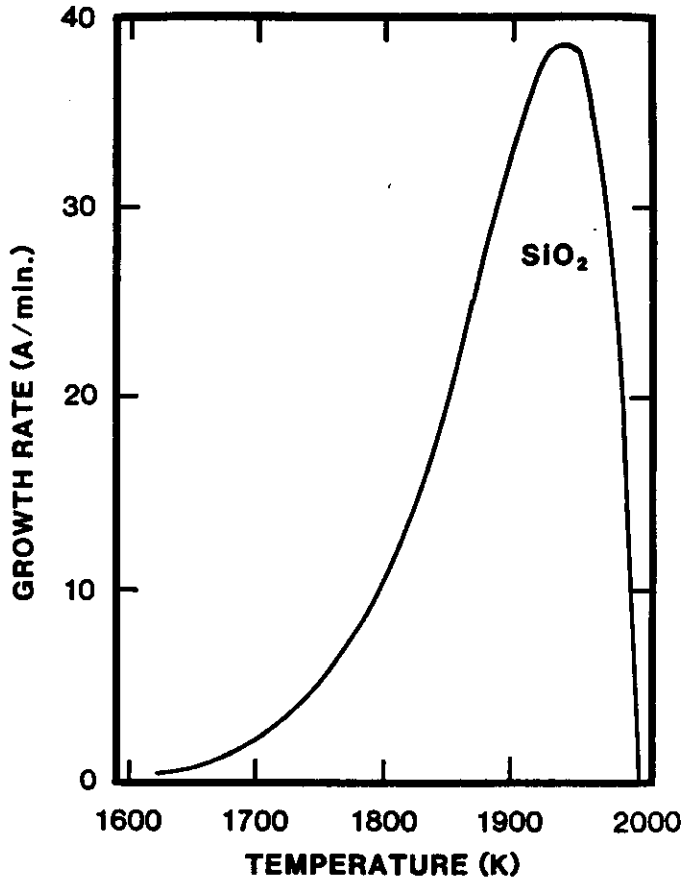

FIGURE 7

Calculated crystal rate, G ($A.min^{-1}$), versus temperature, T(K), for silica (after ref. 17)

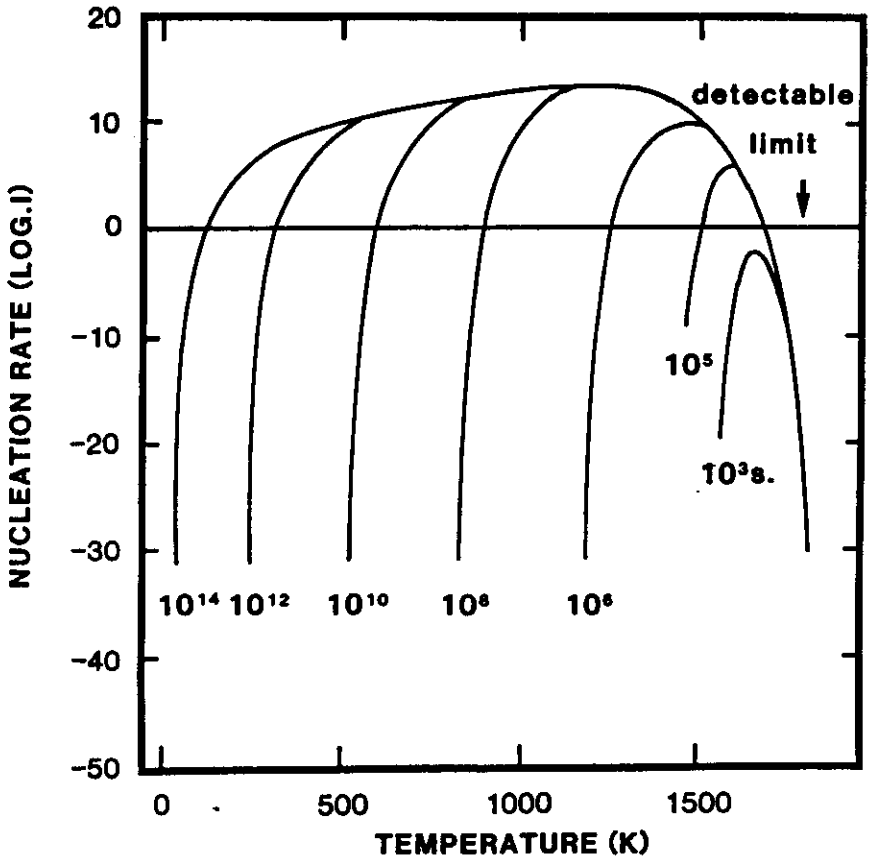

FIGURE 8

Calculated homogeneous nucleation rate, I ($cm^{-3}.s^{-1}$) for silica showing transient effect. Detectable limit is arbitrarily indicated for I = 1 (after ref. 17)

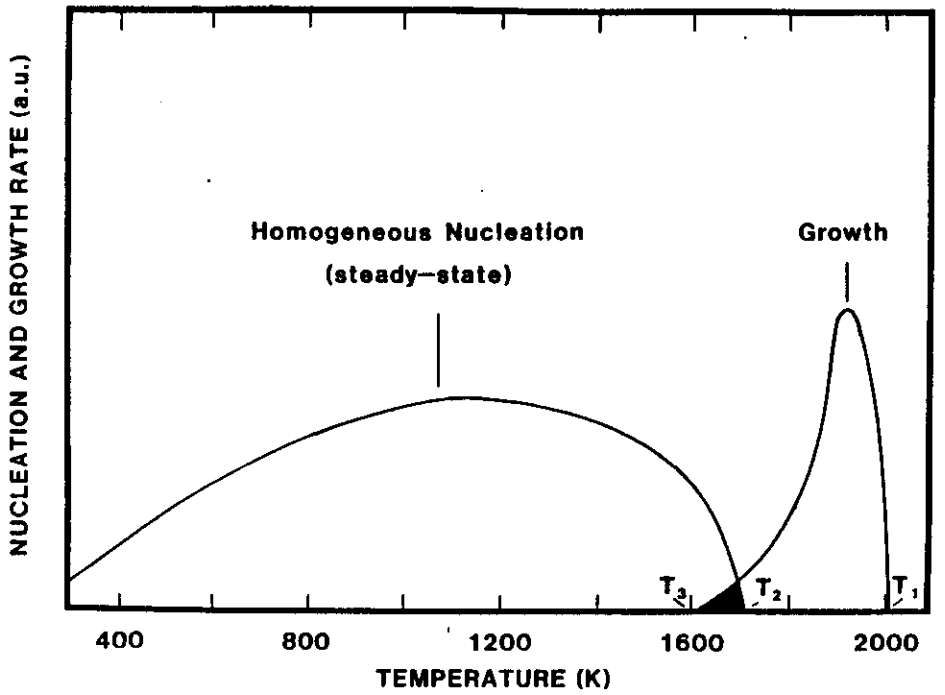

FIGURE 9

Homogeneous nucleation rate, I, and growth rate, G, for silica. The narrow overlap region is shown in dark (after ref. 17)

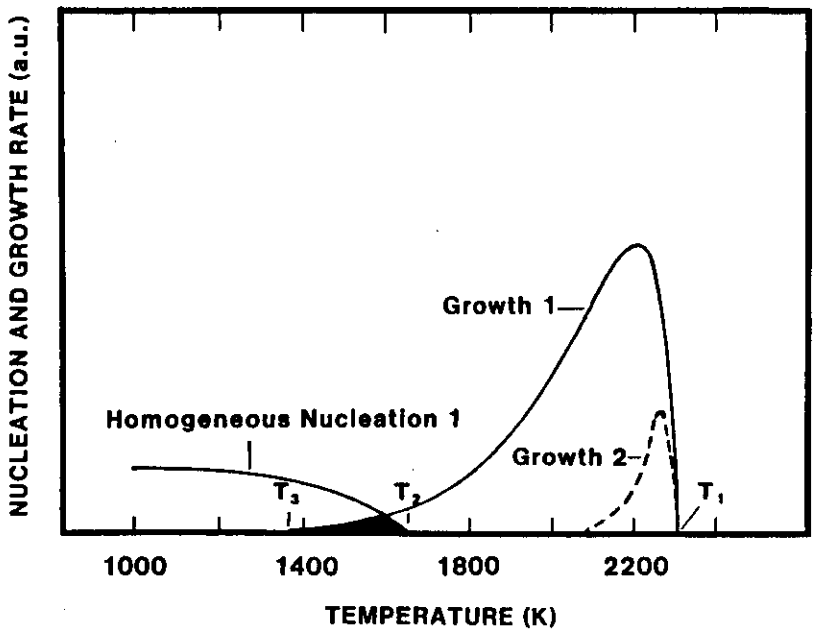

FIGURE 10

Homogeneous nucleation rate, I, and growth rate, G, for alumina (after ref. 17)
1 and 2 indices refer to $d\gamma/dT$ values of SiO_2 and B_2O_3 respectively

The formal theory of transformation kinetics as studied by several authors [17, 18, 19, 20, 21] describes the evolution with time, t, of x in terms of the nucleation frequency per unit volume, I, and the crystal growth rate, G,

$$x(t) = 1 - \exp. \left| k_n \int_0^t I \left(\int_{t'}^t G.dt \right)^n dt' \right| \qquad (56)$$

In this equation, currently referred to as Johnson-Mehl-Avrami (JMA) [21] or Kolmogoroff-Avrami equation, k_n is a geometrical factor which depends on the shape of the growing crystal and n is an integer or half integer which depends on the mechanism of growth and the dimensionality of the crystal.

In the steady-state case, i.e. $\tau = 0$ and I, G constant, equation (56) leads to

$$x(t) = 1 - \exp. \left| [k_n/(n+1)] \; I^s \; G^n \; t^{n+1} \right| \qquad (57)$$

In the non-stationary case, Gutzow and Kashchiev [20] have shown that equation (56) may be written as

$$x(t) = 1 \exp. - [aF(t/\tau)] \qquad (58)$$

where $a = [k_n/(n+1)] \; I^s \; G^n \; \tau^{n+1}$ (59)

and F is a complicated function of t causing the x (t) curve to shift towards longer times.

The ability of an undercooled liquid to effectively bypass crystallization can be appreciated from the critical time, t_c, necessary for the crystallized fraction x to reach a predetermined value, x_c.

Gutzow and Kashchiev have found in the same study that, with the condition $x \ll 1$ of interest in this report, t_c can be approximated as

$$t_c = b\tau + \left| (n+1) \; x_c/k_n \; I^s \; G^n \right|^{1/n+1} \qquad (60)$$

where b is a numerical factor between 0.02 to 0.1.

.../...

The $t_c(T)$ relationship usually plotted in T versus log t_c coordinates is known as Temperature-Time-Transformation (TTT) curve. The TTT equation is a complex expression which can be obtained by recalling equations (24, 42, 46, 60).

Figs 11 and 12 after I. Gutzow et al. [7] are examples of TTT curves for $NaPO_3$ and Ag melts drawn at various ϕ and z_k values for $x_c = 10^{-6}$ and using the VFT equation for η (see other parameters in ref. 7). ϕ is a numerical factor between 0 and 1 which relates to the nucleus shape ; in the case of nuclei having a spherical cap shape, ϕ identifies itself as $f(\theta)$ and $\phi = 1$ for homogeneous nucleation ; $z_k \leq 1$ is a numerical factor accounting for the hindrances accompanying the incorporation of building units into the nucleus ; z_k may take very small values, e.g. 10^{-6} as was experimentally found for the crystallization of the $NaPO_3$ melt [22]. Finally, dotted curves in figs 11 and 12 represent the extreme case where τ is equal to zero.

These very particular examples taken from I. Gutzow et al. illustrate the general properties enunciated below :

Firstly, the kinetic stability of an undercooled liquid is determined by three parameters, namely : the time lag τ, the nucleation rate I and the growth rate G. The incidence of τ on t_c at low ϕ and z_k values is clearly evidenced in figs. 11 and 12.

Secondly, TTT curves give the order of magnitude of the minimum cooling rate, q, necessary for vitrification with a minimal degree of crystallization x_c.

The general criterion for vitrification may be derived from

$$q_c = (T_m - T_n) / t_c(T_n) \qquad (61)$$

where T_n is the temperature of the "nose" of the TTT curve and t_c is given by expression (60) for $T = T_n$ (an approximate solution of equation (61) is given in ref. 7).

.../...

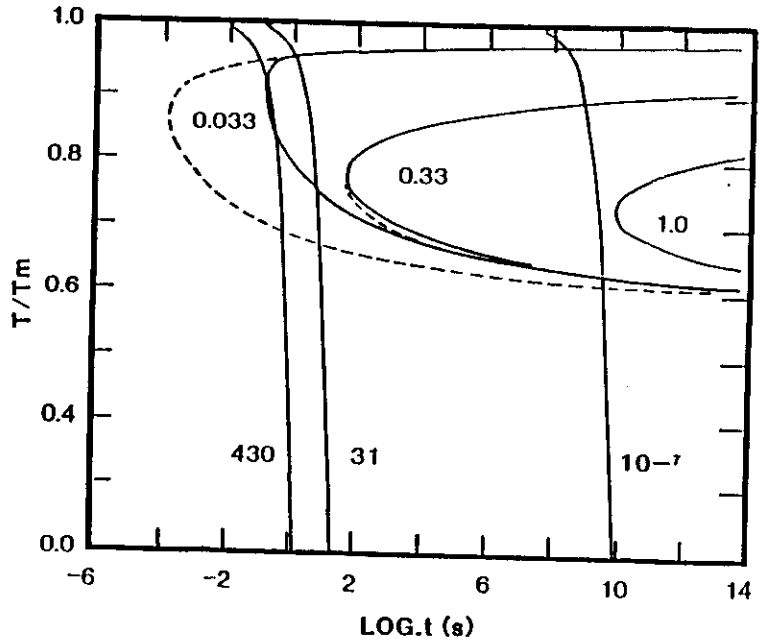

FIGURE 11

TTT curves for $NaPO_3$ melt at various Ø values (as indicated) with the τ-effect accounted (solid curves) and not accounted for (dotted curves). Descending curves correspond to linear cooling rates q (as indicated, $K.s^{-1}$) (after ref. 7)

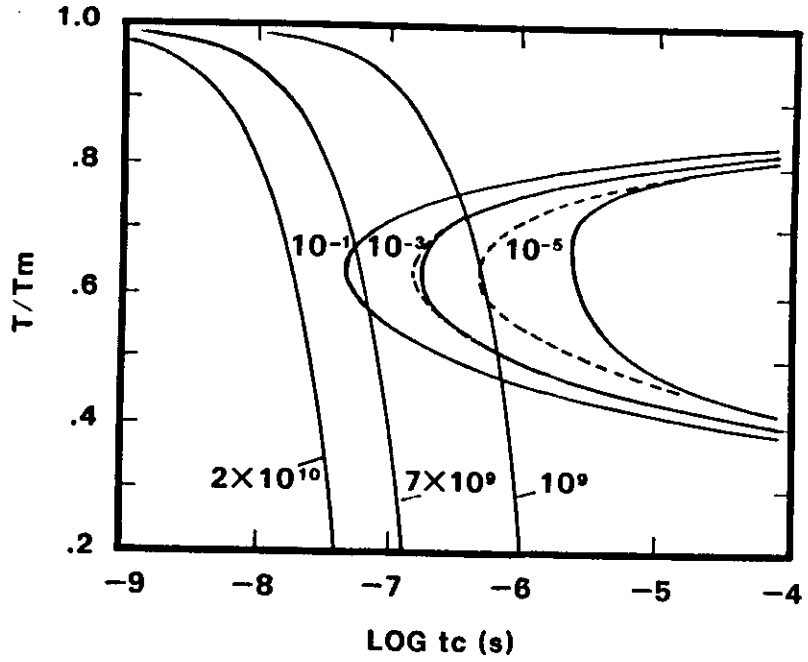

FIGURE 12

TTT curves for Ag melt at various Zk-values (as indicated) with the τ-effect accounted (solid curves) and not accounted for (dotted curves). Descending curves correspond to linear cooling rates q (as indicated, $K.s^{-1}$) (after ref. 7)

The examples in figs. 11 and 12 illustrate extreme values of t_c for homogeneous nucleation (ϕ = 1) and the corresponding q_c values.

Thirdly, at high ϕ values - $\phi \geq 0.3$ - the τ effect is negligible and the TTT curves show a horizontal symmetry axis whereas at low ϕ values they are asymmetrical and the τ effect eventually predominates. The example in fig. 13 is a dramatic illustration of the role of heterogeneous nucleation - especially at low ϕ values - in reducing t_c (T_n) values. From a practical point of view, the asymmetry of a TTT curves is an indication for non stationarity and/or heterogeneous nucleation in the system.

Fourthly, only an extremely good purification of the melt - or liquid - can ensure its vitrification at a rate to the lowest possible one obtainable for homogeneous nucleation (ϕ = 1). This statement follows from the study of q (ϕ) e.g. see fig. 13 [7].

The last point means that homogeneous nucleation sets the upper bound of the critical cooling rate q_c. The knowledge of q_c (hom) is an essential criterion, whenever it is accessible, for the selection of a system for bulk solidification in space. A list of critical cooling rates ($x_c = 10^{-6}$) as estimated by homogeneous nucleation theory for representative systems is given in table 4 [23]. Although some discrepancies have been observed between computed and experimental q_c values, e.g., q_c = 120 K/s. against 1 K/s. experimentally found for the PdNiP glass system [24], this table unambiguously shows that q_c values are spread over orders of magnitude for the different systems ; low q_c values are typical of covalently bonded systems (e.g. silica) and conversely, large q_c values are typical of non-convalently bonded systems, e.g., metals some of which can only be obtained in the form of foils.

II.4 - Complex and multicomponent systems

The concepts of nucleation and growth kinetics developed in the above section strictly apply to single component substances or congruently melting compounds. The liquid-to-solid transformation for these materials only

.../...

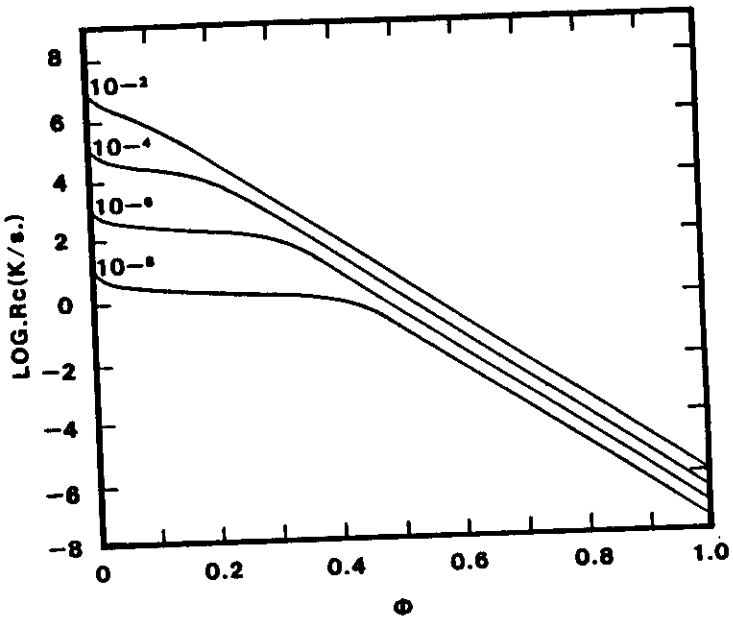

FIGURE 13

Dependence of log q on ϕ for $NaPO_3$ melt at various Zk-values (as indicated) (after ref. 7)

TABLE 4

MATERIAL	q_c (K/s)	Ref.
SiO_2	9.10^{-2}	[25]
Na_2O - 2 SiO_2	6.10^{-3}	[25]
GeO_2	3.10^{-3}	[25]
Salol	2.10^{-2}	[25]
CaO - Al_2O_3 - 2 SiO_2	3.10^{2}	[25]
$Pd_{40}Ni_{40}P_{20}$	$1.2.10^{2}$	[24]
$Ni_{62}Nb_{38}$	$1.4.10^{4}$	[24]
Ge	5.10^{5}	[24]
H_2O	5.10^{5}	[25]
$Fe_{83}B_{17}$	3.10^{6}	[24]
Ni	3.10^{10}	[24]

q_c (K/s) for various glass systems

requires short-range diffusion at the liquid-crystal interface ; the molecule (or formula unit) movements are accounted for by the coefficient of self-diffusion in the bulk liquid. This property validates the use of the Stokes-Einstein equation which links the self-diffusion coefficient to viscosity, viscosity being in most cases more readily attainable than diffusion data.

On the contrary, multicomponent systems cannot be treated that simply since the liquid-to-solid transformation generally involves bond breaking and possibly long-range diffusion processes. This type of transformation is currently termed reconstructive. As pointed our by D.C. Larsen [17], two situations occur whether the transformation is accompanied or not by a large change in chemical composition.

In the case of "network liquids", such as SiO_2, interatomic bonds must be broken prior to the molecular rearrangement just as this is the case for self-diffusion. Thus, the activation energy and diffusion coefficient for "network liquids" can be approximated as for non reconstructive transformations.

When a large compositional change does occur, long-range diffusion processes are necessary to bring the precipitating species at the growth front. In dealing with those problems, Uhlmann and Chalmers [26] suggested that the kinetic barrier to nucleation should be taken as the activation energy for the diffusion of the slowest moving species in the matrix and that the preexponential factor, $\eta\nu$, in equation (15b) should be reduced by the mole fraction of the solidifying species.

Hammel [27] has formulated the volume fraction of material transformed in this kind of reconstructive transformation for diffusion-controlled growth,

$$x = \frac{8\pi}{5} C^3 D^{1/3} I^s t^{5/2} \qquad (62)$$

where D is the diffusion coefficient and C is a supersaturation term.

The major difficulty in both these treatments is that diffusion data are generally unknown and not readily accessible to measurements on earth. Attempts to overcome this difficulty had a limited success so far.

.../...

II.5 - Transformation kinetics, model uncertainties

How fast must a given liquid be cooled in order that detectable crystallization be avoided ? In principle, it appears from the previous chapter that the classical theory of nucleation, if applicable, and the formal JMA theory of transformation kinetics [21] provide the necessary information to estimate the critical conditions, for forming a glass from a given material. This information is contained in the TTT curves drawn from the JMA expression (56), recalled below

$$x(t) = 1 - \exp\left[-\left| k_n \int_0^t I \left(\int_{t'}^t G\,dt \right)^n dt' \right|\right]$$

In practice, however, information on the temperature dependence of the nucleation frequency and of the growth rate are seldom available. Therefore, as proposed by D.R. Uhlmann, it is generally convenient to estimate the nucleation rate, I, and the growth rate, G, from standard theoretical models using simplifying hypotheses. Thus, D.R. Uhlmann proposes for I the expression [28] :

$$I^S = C \cdot \nu_n \cdot \exp\left(-\frac{0.0205\ B T_m^5}{T^3\ \Delta T^2}\right) \qquad (63)$$

where C is a constant ($\sim 10^{30}\ cm^{-3}.s^{-1}$ P) and B is the free energy of formation of the critical nucleus in units of kT* with $T^* = 0.8\ T_m$.

Recalling the expression (46) of the growth rate, G,

$$G = f_{gs}\ \nu_g \left| 1 - \exp\left(-\frac{\Delta G_m}{RT}\right) \right|$$

and using the customary relation

$$\nu_n = \nu_g = \frac{kT}{3\pi\lambda^3\eta} \qquad (64)$$

it is possible to derive approximated JMA expressions and in turn, to calculate TTT curves.

.../...

The application of this approach to particular systems, e.g. classic network oxides, SiO_2 and GeO_2, an organic liquid, phenyl acetate (Salol) and metals has been made with some success by D.R. Uhlmann for the case of homogeneous nucleation. As pointed out by this author, the greatest uncertainty in these calculations lies in the estimate of nucleation frequencies. These estimates should not be taken as accurate to better than up to eight orders of magnitude corresponding to 1 to 2 orders of magnitude in terms of calculated critical cooling rate, q_c.

This uncertainty on q_c, acceptable for a classification of the different compound families with respect to their glass-forming ability, is no more acceptable when the range of predicted intrinsic q_c values contains the limits of q values practically achievable from a technological point of view.

In the recent years, a number of quantitative studies on nucleation kinetics have been made on glass forming systems having a simple composition. A simple composition is defined as one in which the crystallizing phase has the same composition as the parent glass, which includes congruently-melting compounds. A review of this work was recently made by P.F. James [29]. Similar reviews on crystal nucleation in more complex systems are also available (see ref. articles in [5]).

Quantitative analyses of transformation kinetics are most often based on the steady-state and transient nucleation rates as formulated by Kashchiev - e.g. expressions (15) & (42). The thermodynamical data used in these treatments primarily involve the driving force, ΔG_v, for crystallization, viscosity, η, and the specific free energy, σ, at the crystal/melt interface.

The general expression of the bulk free energy change per mole upon crystallization, ΔG (in relation 3b) is given by

$$\Delta G = -\Delta H_f (T_m - T)/T_m - \int_T^{T_m} \Delta Cp\ dT + \int_T^{T_m} (\Delta Cp/T)\,dt \qquad (65)$$

.../...

where ΔH_f is the heat of fusion per mole, T_m is the melting temperature and ΔCp is the difference in specific heats between the crystal and the liquid at temperature T.

Substitutes for expression (65) are currently used in order to overcome the lack of data on ΔCp, e.g.,

$$\Delta G_v = - \Delta H_f (T_m - T)/T_m, \quad (\Delta Cp = 0) \tag{66}$$

and Hoffmann's expression [30],

$$\Delta G_v = - \Delta H_f (T_m - T)/T_m^2 \tag{67}$$

Viscosity, η, is introduced in the I^s expression (21) via the Stokes-Einstein relation $D = kT/3 \pi \lambda \eta$ in order to circumvent the absence of data on effective diffusion coefficients.

The $\eta(T)$ relation was studied theoretically for the hard sphere model by Cohen & Turnbull [31] and in the case of chain polymer melts by Bueche [32]. The expression of $\eta(T)$ currently retained is the well-known Vogel-Fulcher-Tammann equation

$$\eta = A \exp (B/(T - T_o)) \tag{68}$$

where A, B and T_o are constants depending on the material and T is the absolute temperature. (T_o is the temperature below which the relative free volume of the fictive supercooled liquid, as defined in the "hole theory of liquids", becomes zero). This is the case of silica with an activation energy of the order of the chemical bond energy of the structure [14]. In contrast, the viscosity of many glass formers is characterized by low B values and T_o's which are a large fraction of T_m when compared with silica. The specific free energy at the crystal/liquid surface, or surface tension, σ, is a function of temperature which may be expressed as

$$\sigma(T) = \sigma(T_m) + s(T) \tag{69}$$

where $\sigma(T_m)$ is the value of σ at the thermodynamical melting temperature,

T_m and $s(T)$ is a complexed function of temperature often reduced to its linear form $s(T) = a\,T$. $\sigma(T_m)$ is given by the semi-empirical Scapski-Turnbull formula [33]. This brief review of the thermodynamical data involved in I^s and $I(t)$ expressions suggests that large uncertainties are expected in quantitative analyses.

Indeed, this is reflected in plots of $L_n (I\eta/T)$ against $1/\Delta G_v^2.T$ which should, according to nucleation theory, produce a straight line, the slope yielding σ and the intercept yielding the pre-exponential factor A ($A \simeq Nk/3\pi\lambda^3$) in a simplified form of expression (21)). Such plots established for a number of simple glass-forming systems, e.g., $Li_2O - 2\,SiO_2$ and $BaO - 2\,SiO_2$ [5] actually produce a good straight line fit over most of the nucleation temperature range. However, the experimental values of A derived from the intercept of the plot differ from the predicted ones by orders of magnitude - over 20 orders of magnitude higher for the two systems above. This discrepancy cannot be ascribed to the simplifying hypotheses made to derive A, and thus it does not necessarily invalidate the classical theory of nucleation ; it may simply reflect the large uncertainties on η, ΔG_v and eventually σ values.

This situation is worse in the case of complex glass-forming systems where the crystallizing species have a composition which differs from that of the liquid ; in this case, the identification of the first crystallizing species is an additional difficulty which must be unambiguously solved out for quantitative analysis purposes.

A better assessment of the validity of the classical theory of nucleation and a more accurate exploitation of its predictions where it is applicable, whatever the glass-forming system, requires important investigations in the following directions :

i) acquisition of the exact thermodynamic expression of ΔG,
ii) measurement of the effective coefficients involved in the crystallization process,
iii) assessment of the $\sigma(T)$ relation and of the limit of validity of the capillary model - extension to atomistic models ?

.../...

Eventually, these analyses could be aided considerably where transient nucleation is important using numerical simulation by computer as proposed by K.F. Kelton et al.

It is essential to point out - owing to the general objective of this report - that the microgravity environment procures unique possibilities for the accurate determination of diffusion coefficients as indicated in the previous chapter. This new possibility would make the use of the Stokes-Einstein equation unnecessary.

.../...

LIST OF REFERENCES

[1] M. Volmer and A. Weber, Z. Phys. Chem. 119 (1926) 227.

[2] D. Turnbull and J.C. Fischer, J. Chem. Phys. 17 (1949) 71.

[3] A.G. Walton, "Nucleation in liquids and solutions", chapter in Nucleation, A.C. Zettlemoyer, ed., (Marcel Dekker, NY 1969).

[4] K.F. Kelton, A.L. Greer and C.V. Thompson, J. Chem. Phys. 79 (12) (1983) 6261.

[5] E.D. Zanotto and P.F. James, J. of Non Cryst. Sol. 74 (1985) 373.

[6] P.F. James, J. of Non Cryst. Sol. 73 (1985) 517.

[7] I. Gutzow, D. Kashchiev and I. Avramov, J. of Non Cryst. Sol. 73 (1985).

[8] J.B. Zeldovich, Acta Physico-Chim., URSS 18, 1 (1943).

[9] J. Frenkel, Kinetic theory of liquids (Oxford University, Oxford, 1946).

[10] D. Kashchiev, Surface Sci. 14 (1969) 209.

[11] I. Gutzow, in : 1976 Crystal Growth and Materials, eds. E. Kaldis and H.J. Scheel (North Holland, Amsterdam, 1977) p. 380.

[12] D.R. Uhlmann, in : Advances in Ceramics, Vol. 4, Nucleation and Crystallization in Glasses, eds. J.H. Simmons, D.R. Uhlmann & G.H. Beall (Amer. Ceram. Soc., Columbus, Ohio 1982), p. 80.

[13] D. Turnbull, Trans. AIME, 221 (1961) 422.

[14] D. Turnbull, Contemp. Phys. 10-5 (1969) 473.

[15] G.S. Fulcher, J. Am. Ceram. Soc., 6 (1925) 339.

[16] H. Yinnon & D.R. Uhlmann, J. of Non Cryst. Sol. 54 (1983) 253.

[17] D.C. Larsen, Nasa Contract NAS8-29850.

[18] A.N. Kolmogoroff, Bull. Acad. Sci. URSS (Sci. Mat. Nat.) 3 (1937) 355.

[19] M. Avrami, J. Chem. Phys. 7 (1939) 1103 ; 8 (1940) 212 ; 9 (1941) 177.

[20] I. Gutzow & D. Kashchiev, Commun. Dept. Chem. (Bulg. Acad. Sci.) 3 (1970) 315.

.../...

[21] W.A. Johnson & K.F. Mehl, Trans. Am. Inst. Mining Met. Engns. 135 (1981) 315.

[22] I. Gutzow & S. Toschev, Kristall und Technik 3 (1968) 485.

[23] J. Zarzycki, G.H. Frischat, D.M. Herlach, in : Fluid Sciences & Materials Science in Space, ed. H.U. Walter, ESA Publication, (Springer-Verlag 1987) 599.

[24] H. Scholze : Glas, 2nd edition (Springer Verlag 1977) 67.

[25] P.I.K. Onorato & D.R. Uhlmann, J. Non Cryst. Sol. 22 (1976) 367.

[26] D.R. Uhlmann & B. Chalmers, "The energetics of nucleation", Nucleation Phenomena, Am. Chem. Soc. (1966).

[27] J.J. Hammel, "Nucleation in glass forming materials", chapter in Nucleation, A.C. Zettlemoyer ed. (Marcel Dekker, NY 1969).

[28] D.R. Uhlmann, in : Materials Science Research, Vol. 4 (Plenum, New-York, 1969).

[29] P.F. James, in : Advances in Ceramics, Vol. 4, eds. J.H. Simmons, D.R. Uhlmann and G.H. Beall (Am. Ceram. Soc. Inc. Columbus, Ohio, 1982), p. 1.

[30] J.D. Hoffman, J. Chem. Phys. 29 (1958) 1192.

[31] M.H. Cohen and D. Turnbull, J. Chem. Phys. 31 (1959) 1164.

[32] F. Bueche, Physical Properties of Polymers (Interscience, New-York, 1962), 85.

[33] J.H. Hollomon and D. Turnbull, in : Progress in Metal Physics, Vol. 4, ed., D. Chalmers (Pergamon, London 1953).

FIGURE CAPTIONS

1 - Heterogeneous nucleation : stability of an embryo of radius R on a substrate ; θ is the wetting angle.

2 - Surface-controlled growth mechanism.

3 - Example of calculated variation against temperature of the steady-state nucleation rate, I, (in $cm^{-3}.s^{-1}$, homogeneous case) in an undercooled liquid for various values of the parameter $\alpha\beta^{1/3}$. The expression of I is given in the figure (after ref. 14).

4 - Example of calculated variation against temperature of the homogeneous nucleation rate I (see fig. 3) for $\alpha\beta^{1/3}$ = 0.5 and 3 Trg values (after ref. 14).

5 - Measured nucleation rate, I, and growth rate, G, in anorthite system. A substantial overlap of the two processes is clearly visible (after ref. 16).

6 - Nucleation rates and growth rate of a hypothetical system. T_m is the melting point.

7 - Calculated crystal rate, G ($nm.s^{-1}$), versus temperature, T(K), for silica (after ref. 17).

8 - Calculated homogeneous nucleation rate, I ($cm^{-3}.s^{-1}$) for silica showing transient effect. Detectable limit is arbitrarily indicated for I = 1 (after ref. 17).

9 - Homogeneous nucleation rate I, and growth rate, G, for silica. The narrow overlap region is shown in dark (after ref. 17).

10 - Homogeneous nucleation rate, I, and growth rate, G, for alumina (after ref. 17).

11 - TTT curves for $NaPO_3$ melt at various ϕ values (as indicated) with the τ-effect accounted (solid curves) and not accounted for (dotted curves). Descending curves correspond to linear cooling rates q (as indicated, $K.s^{-1}$) (after ref. 7).

12 - TTT curves for Ag melt at various Zk-values (as indicated) with the τ-effect accounted (solid curves) and not accounted for (dotted curves). Descending curves correspond to linear cooling rates q (as indicated, $K.s^{-1}$) (after ref. 7).

13 - Dependence of log q on ϕ for $NaPO_3$ melt at various zk values (as indicated) (after ref. 7).

III - INDUSTRIAL PERSPECTIVES IN ADVANCED GLASSES

III.1 - Applications

Advanced glass technology increasingly expands by including borderline glass systems in order to meet the demands of industry. This interest for glasses follows from the fact that i) glasses have properties which are superior in many situations to those of their crystalline counterparts and ii) glasses have an enormous compositional potential as compared with crystalline materials. In addition, glasses can virtually be used in any shape. They progressively enter all sectors of advanced technologies ; the non-exhaustive list below illustrates the diversity of these applications :

. Refractive optics/visible and infra-red transmitters :
  - aplanats,
  - long focal length lenses,
  - spectrometers,
  - high-speed large lens, etc...

. Laser hosts.

. Optical waveguide :
  - telecommunications,
  - laser energy transport,
  - sensors.

. Devices/transducers :
  - magneto-optic recording,
  - optical recording,
  - electrophotographic recording,
  - optical non-linear devices (bistable devices, optical switches, etc...).

. Sensors :
  - bolometers.

.../...

. Permanent magnet materials.

. Corrosion-resistive coatings.

. Glass-ceramic composites, etc...

A list of some major glass systems which fall into these fields of applications is given in table I. It is not intended here to develop the industrial perspectives for advanced glasses within each category of applications. Firstly, the discussion will be restricted to selected, comprehensive examples, namely : refractive optics, optical telecommunications and lasers. Secondly, film technologies on the one hand and amorphous metals or alloys, which require extreme cooling rates for their formation, are not relevant of GPS and will not be considered in this section.

III.1.1. Refractive optics/visible transmitters

The principal characteristics of glasses of interest for refractive optics are, besides transparency :

1/ the index of refraction, n,
2/ the dispersion, $dn/d\lambda$,
3/ the optical isotropy.

The shaded area in fig. I, after Happe, encloses the n, ν values explored thus far for commercially available glasses [1]. ν is the Abbe number defined as :

$$\nu_D = (n_D - 1) / (n_F - n_C) \qquad (1)$$

which varies in inverse relationship to the dispersion $dn/d\lambda$. In relation (1), n_D, n_F and n_C are the indices of refraction of the glass for the blue hydrogen F line, the yellow sodium D line and the red hydrogen C line respectively. The data given in this figure for crystalline materials, e.g., Al_2O_3 and ZrO_2, are mean index values $\bar{n}$ calculated by the formulas :

$$\bar{n} = \frac{1}{3}(2\omega + \varepsilon) \quad \text{or} \quad \frac{1}{3}(\alpha + \beta + \gamma)$$

.../...

TABLE I

Some major glass families

OXIDES

- Silicates
- Germanates
- Borates
- Aluminates
- Gallates
- Phosphates
- Oxynitrides
- Tellurates
- Heavy metal oxide glasses, etc...

HALIDES

- Berrylides
- Zirconides
- Fluorophosphates
- Fluoroaluminates
- Heavy metal fluoride glasses, etc...

CHALCOGENIDES

- Arsenides
- Selenides, etc...

CHALCOHALIDES

- Tellurides

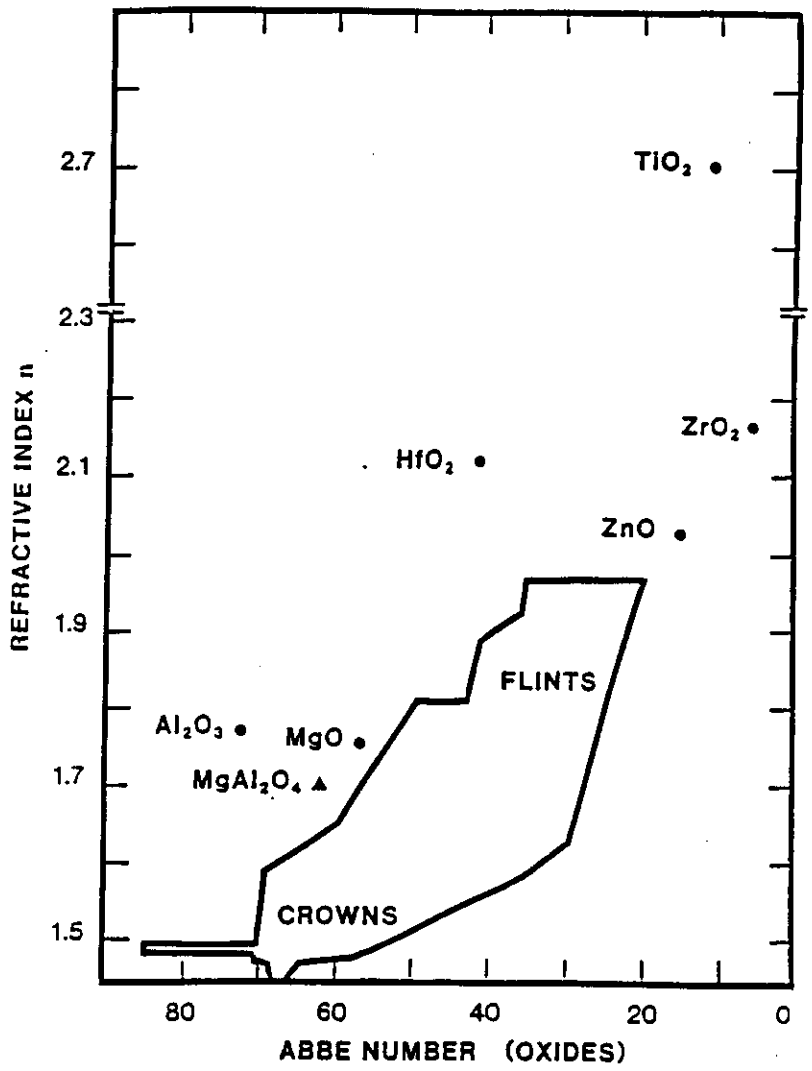

FIGURE 1

Refractive index versus Abbe number for oxides. The enclosed area relates to commercial glasses, after ref. 1

where ω, ε, α, β and γ stand for the ordinary and extraordinary rays of uniaxial crystals and the 3 rays of biaxial crystals respectively. It appears in fig. 1 that past glass technology for refractive optics was restricted to a band which links low-index/low- dispersion (crown) glasses to high index/high dispersion (flint) glasses. Table 2 lists some pertinent optical properties on the visible range of the spectrum of a number of transparent crystalline oxides which fall out of this band.

For the preparation of optical systems, highly corrected for chromatic aberrations, it is desirable to expand this band to the high-index/low-dispersion direction and it is indispensable to dispose of materials having different dispersion characteristics.

The achievement of glassy materials reproducing the high-index/low-dispersion properties of spinel $MgAl_2O_4$ or corundum Al_2O_3 may be within reach. Indeed, laboratory experiments have shown that Y_2O_3, Sm_2O_3, Ga_2O_3 [2] and $Y_3Al_5O_{12}$ [3] (YAG in the crystalline state) could be solidified in the glassy state. These results were obtained on spheres typically a few millimetres in diameter levitated in a vertical gas stream throughout fusion - obtained by means of a CO_2 laser - and subsequently allowed to cool down.

Materials having different dispersions are necessary to correct the flaw, known as secondary spectrum, i.e. the residual chromatic aberration which remains after two wavelengths have been brought to a common focus using conventional achromatization techniques. The secondary spectrum, L, is a function of the dispersion ratios, P_i, and the Abbe numbers, ν_i, of the optical material, i, used in the system. For a two-component achromat, the secondary spectrum, L, is specified as

$$L = f\,[(P_1 - P_2) / (\nu_1 - \nu_2)] \qquad (2)$$

where f is the focal length, $P_1(2)$ is the partial dispersion ratio and $\nu_1(2)$ the Abbe number of component 1 (2). P terms are currently given for visible transmitters by the expression

$$P = (n_F - n_D) / (n_F - n_C) \qquad (3)$$

.../...

TABLE 2

Optical properties of some oxides,
after a bibliographic study of R.A. Happe [1]

Oxide	Structure	Ray	n_D	ν_D (calculated)
Al_2O_3	Rhombohedral (corundum)	ω	1.7686	71.8
		ε	1.7604	73.1
CeO_2	Cubic (film, polycryst)		2.148	8–10
HfO_2	Monoclinic	α	2.070	37
		β, γ	2.146	44
$MgAl_2O_4$	Cubic		1.72	63
MgO	Cubic		1.73790	54.3
Nb_2O_5	Unknown (film data)		2.258	8
Ta_2O_5	Unknown (film data)		2.091	23
TiO_2	Tetragonal (rutile)	ω	2.6124	10.5
		ε	2.8993	9.3
	Unknown (film data)		2.657	9
ZnO	Hexagonal (zincite)	ω	2.013	15.8
		ε	2.029	14.9
ZrO_2	Monoclinic	α	2.13	~ 5
		β	2.19	
		γ	2.20	

In order to minimize L, $(P_1 - P_2)$ should be small and $(\nu_1 - \nu_2)$ large. In practice however, it is found that the P, ν relationship of glasses of a given base falls on a straight line, fig. 2. Thus, it is necessary to choose glasses of more than one base for the individual elements of the lens. For this reason, borate and phosphate-based glasses enter with silica-based glasses in the composition of the elements of sophisticated achromats.

Nevertheless, as this qualitatively appears in fig. 2 , the displacements of the P, ν curves are small for the different bases. Further reduction of the secondary spectrum may be achieved by i) expanding the P, ν relationship in the phosphate and borate glass families - possibly by exploring borderline compositions in these families - and ii) identifying new glass-forming families able to produce new P, ν relationships. Finally, the growing interest for infrared-based technology should stimulate the search for new optical materials in this region, e.g. chalcogenide glasses with increased silicon and germanium contents to improve their stiffness and chemically durable halide glasses.

III.1.2. Lasers

Of the various applications of glasses in laser technology, the development of large, high-power neodynium-glass lasers for Inertial Confinement Fusion (I.C.F.) experiments is most demanding. This application is a good example of both the extreme requirements imposed on optical materials and the considerable potential of glasses to meet these requirements.

The Shiva laser at Lawrence Livermore Laboratory, operational since November 1977, can provide 30 TW on a target typically less than 100 μm in diameter at a submicron wavelength and for a pulse duration of typically one nanosecond. This laser uses a Nd^{3+}- CaO rich silicate glass. The second generation Nova laser based on a fluorophosphate host glass is ten times more powerful.

.../...

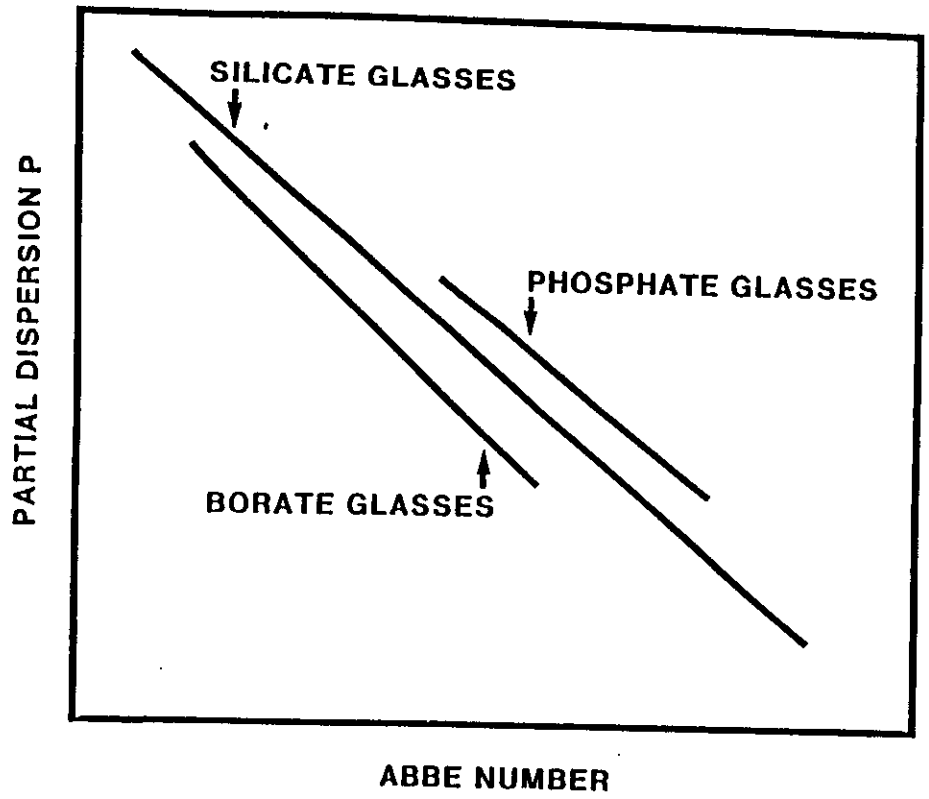

FIGURE 2

Schematic of partial dispersion P versus Abbe number for borate, silicate and phosphate glasses, after ref. 1

The selection of the host glass compromises opposing constraints of chemical, thermomechanical and optical origins. A series of papers give detailed accounts of the problems relevant of this technology, e.g. [4 to 6]. Some crucial optical aspects are briefly discussed below.

Besides the usual problems of chemical durability and mechanical strength, major concerns relate to extrinsic properties such as optical heterogeneities or damaging inclusions and intrinsic properties, namely i) the non-linear terms in the material polarizability and ii) the spectroscopic properties of the active lasing ion in its glass host.

Inclusions are generally submicronic particles introduced during the fabrication step, which may cause the glass to crack under intense irradiation by simple thermomechanical effect. Considerable efforts have been devoted to the elimination of platinum such particles in silica-based glasses processed in platinum crucibles and aimed at laser applications [7].

From the optical point of view, the host glass composition must compromise the demand for low values of the non-linear index of refraction and a high laser efficiency.

The non-linear term of the material polarizability is reflected in the refractive index n by the term Δn,

$$n = n_o + \Delta n \qquad (4)$$

where n_o is the usual linear index and Δn is the intensity-dependent index change. For a laser beam of intensity I, the index change Δn is given by

$$\Delta n = n_2 \langle E^2 \rangle \quad \text{or alternatively}$$
$$\Delta n = \gamma I$$

where $\langle E^2 \rangle$ is the mean-square of the amplitude E of the optical electric field.

.../...

n_2 can be conveniently linked to the linear index n_D and the Abbe number by the empirical relationship [8] :

$$n_2 \ (10^{-13} \ \text{e s u}) = \frac{68 \ (n_D - 1) \ (n_D^2 + 2)^2}{[1{,}517 + [(n_D^2 + 2) \ (n_D + 1)] \ \nu / 6 \ n_D]^{1/2}} \qquad (5a)$$

with also

$$\gamma (\text{m}^2/\text{W}) = \left(\frac{40\pi}{c n_D}\right) n_2 \ (\text{e s u}) \qquad (5b)$$

where c is the speed of light in vacuo.

This non-linearity phenomenon can be overcome by appropriate design of the beam profile. However, it is no more controllable at material imperfections : foreign particles, e.g., bubbles or optical heterogeneities, where local intensity fluctuations may occur. The consequences of these local intensity-dependent changes in the refractive index are changes in the beam divergence with a loss of focusable energy and eventually, catastrophic damage to the material.

Thus, refractive index non-linearities are among the most serious limitations to high-power laser performance. Table 3 and fig. 3 after M.J. Weber et al [8] give a series of γ values for typical glass families and lines of constant γ values for known glasses in the n_D, ν diagramme respectively.

In agreement with the empirical expression of n_2 (and alternatively γ), these data indicate that the best glass candidates for high-power laser technology are low-index, low-dispersion glasses, i.e. glasses containing low-atomic number cations and in which oxygen is replaced by fluorine.

The spectroscopic properties of the Nd^{3+} lasing ion are affected by the glass former network and within a glass family, by the network modifications. Thus, the composition of the glass can be tailored to optimize the relevant spectroscopic properties.

.../...

TABLE 3

Non-linear refractive index coefficients of glasses measured interferometrically using linearly polarized 1064-nm laser pulses, after a bibliographic study of M.J. Weber et al., ref. 8

Glass	Type	n_D	$\gamma(10^{-20}$ m²/W)
Fused silica	4000	1.458	2.73 ± 0.27
Beryllium fluoride	BeF_2	1.275	0.75 ± 0.10
Silicate	SF-6	1.805	21.2 ± 2.1*
Borosilicate	BK-7	1.517	3.43 ± 0.34
Fluorosilicate	FK-5	1.487	3.01 ± 0.30
Fluorophosphate	FK-51	1.487	1.94 ± 0.19

The development of the Shiva and Nova laser host glasses is indicative of the evolution of glass technology. The laser host glass retained for the Shiva laser was a silica-based glass. It was found that in this glass family, the laser efficiency increased with the Ca^{2+} modifier concentration but at the same time the tendency to devitrification increased [9]. This glass family was superseded by the fluorophosphate glass family with the Nova project for its lower n_2 values, typically 0.55 x 10^{-13} esu against $1.5.10^{-13}$ esu for silica-based glass [6].

Fluorophosphate used in the Nova laser are located in the upper right half of the fluoride glass region in fig. 3. It appears that further progress may be obtained with fluoroberyllate glasses.

The general trend in the particular high-power laser technology evolves in the direction of borderline compositions characterized by a high toxicity, chemically reactive species and a tendency to devitrification. The spectroscopic properties of the lasing ion and the n, ν relationship cannot presently be theoretically predicted for a given glass composition so that these essential data must be obtained experimentally. It is worth observing in the context of this report that samples 1 cm^3 in size are sufficient for such investigations.

III.1.3. Optical waveguides

Research on mid-IR optical fibres has been so far mostly concentrated on ultra-low loss fibres for optical telecommunications. The first generation fibres - based on silicate glasses - has already attained the minimum theoretical attenuation loss of 0.16 dB/km at 1.55 μm and considerable interest is now directed towards the extension of this technology to longer wavelengths in the infra-red.

Heavy Metal Fluoride Glasses (HMFG's) based on ZrF_4, discovered by M. Poulain, J. Lucas and co-workers [10], are currently considered to be the primary material for the next generation of optical communication fibres for i) their higher transparency as compared to oxide and chalcogenide glass families and ii) their superior glass forming ability with respect to the other halide glasses.

.../...

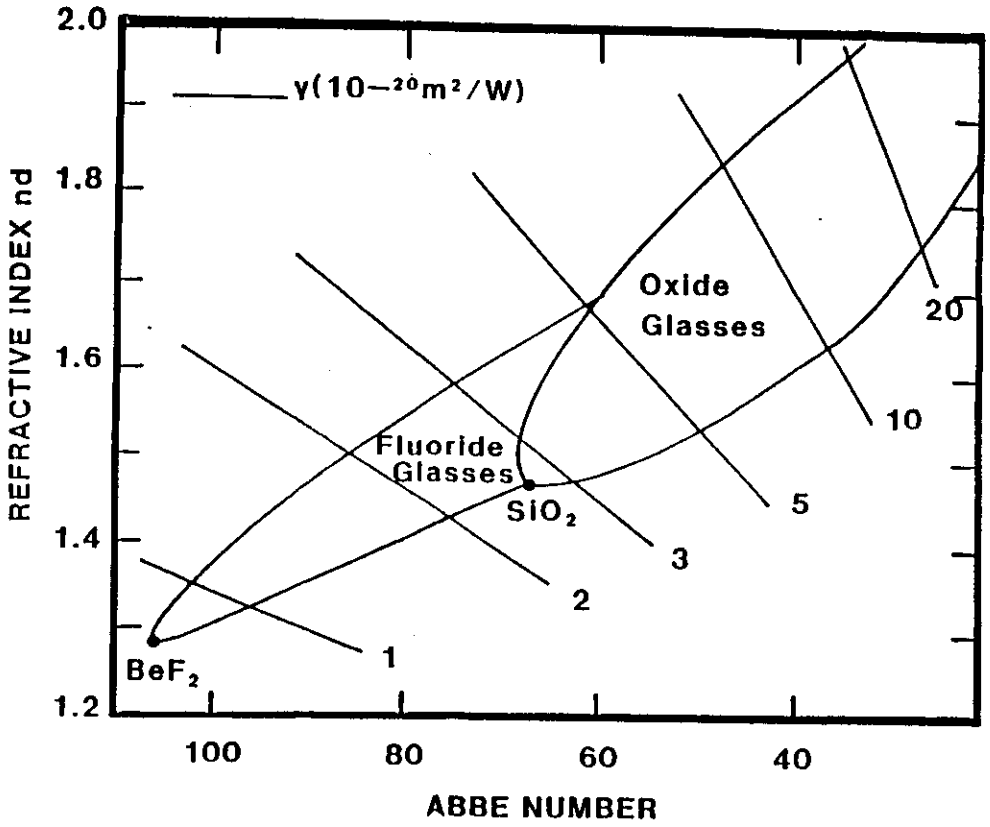

FIGURE 3

Known regions of refractive index and reciprocal dispersion (Abbe number) of optical glasses. Lines of constant γ at long wavelengths have been estimated from equations 5a-b, after ref. 8

The predicted intrinsic minimum attenuation in ZrF_4-based HMFG's is $\sim 10^{-3}$ dB/km at 3.44 µm as compared to 0.16 dB/km for silica and $\sim 10^{-2}$ dB/km at 4.54 µm for chalcogenide glasses, fig. 4. Such low attenuations offer the prospect of repeaterless transoceanic or trans-continental optical links - not to mention other applications, still in the research stage, e.g., laser fibres.

A voluminous literature has concentrated on the properties and elaboration problems of HFMG's, e.g. refs. 10 to 12. The following is intended to provide the necessary background for a comprehensive evaluation of the interest of GPS in this area.

Three prerequisites of primary importance for HFMG-based optical fibres relate to :

i) the stability of the glass
ii) the control of the refractive index
iii) the elimination of loss factors in order to reach the theoretical attenuation limit.

The stability of the glass is crucial for the successive technological steps of the fibre fabrication, e.g., preform preparation and fibre drawing, where the material is processed in the critical Tg, Tm temperature range. The glass stability is conveniently described by the critical cooling rate, q_c, which represents the lowest cooling rate without crystallization. Table 4 after T. Kanomori [13] gives q_c values for different HMFG's ; it is seen that these values expand from several tens of degrees Kelvin per minute (K/min) for early-developed fluoride glass systems of ZBLA (ZrBaLaAl-F) formulation to a few K/min for ZBLAN glasses where N stands for sodium.

The obtention of low q_c values indicates that fluoride glasses may offer reasonable stability, similar to that of oxide glasses, for the envisaged applications. Thus far, improved stability has been obtained by empirical adjustments of the glass formulation and by the control of the ambient atmosphere. However, the optimization of glass stability by means of compositional changes is often balanced by detrimental effects regarding for instance the mechanical strength, the chemical durability, the refractive index and the attenuation of the fibre.

.../...

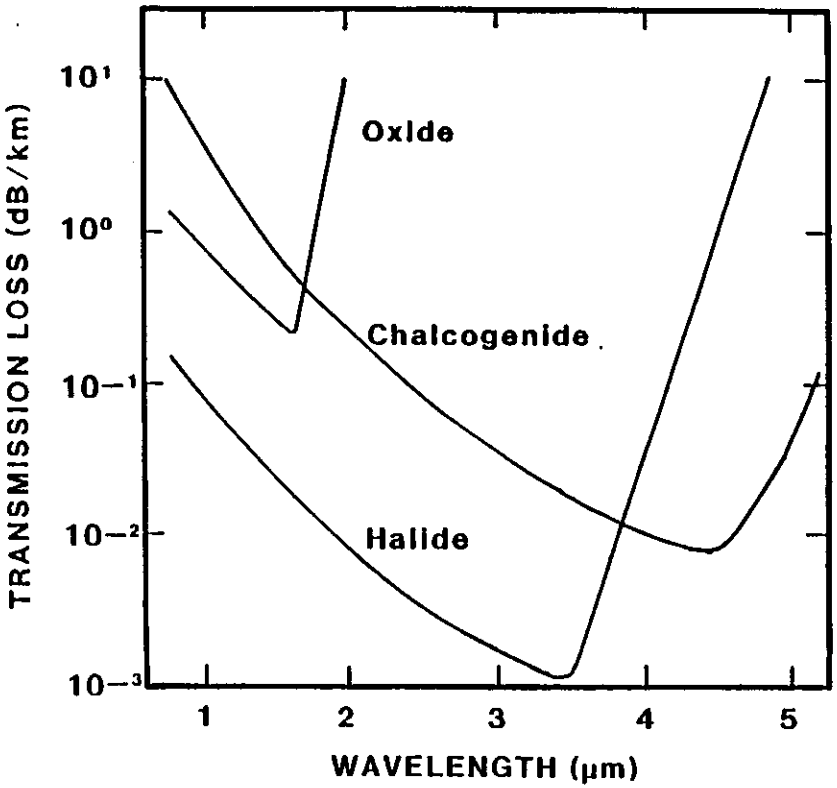

FIGURE 4

Intrinsic optical attenuation of various glass families, after T. Manabe

TABLE 4

Critical cooling rate q_c for typical fluoride glasses

GLASS	ZrF_4	BaF_2	GdF_3	LaF_3	YF_3	AlF_3	LiF	NaF	q_c (K/min)
ZBG	63	33	4	-	-	-	-	-	370
ZBGA	60	32	4	-	-	4	-	-	70
ZBLAL	52	20	-	5	-	3	20	-	26
ZBLYAL	49	22	-	3	3	3	20	-	26
ZBLAN	51	20	-	4.5	-	4.5	-	20	0.7
ZBLYAN	47.5	23.5	-	2.5	2	4.5	-	20	1.1

Thus, alkali halides improve glass forming ability and glass resistance to corrosion but they degrade its chemical durability. Similarly, additions of AlF_3 increase the fibre toughness on the one hand but they displace the multiphonon absorption edge towards low wavelength values (λ) and stimulate phase separation on the other hand. Finally, low concentrations of LaF_3 favour devitrification whereas high concentrations give LaF_3 precipitates during quenching.

A number of experimental facts also strongly suggest that the atmosphere - reducing, oxidizing or containing water - eventually contributes to the formation of heterogeneous nucleation sites, concomitantly with the melt container walls or oxide particles originating from the raw materials.

Despite the considerable amount of material published on HMFG's transformation, the present understanding of nucleation-crystallization in these materials relies on empirical studies which relate the glass forming ability to phenomenological parameters. Thus, there is no quantitative assessment of the intrinsic q_c values of halide glasses. A theoretical approach of q_c values based on classical nucleation theory, if applicable, is complicated as in all multicomponent systems by the lack of relevant thermodynamical data, among which the diffusion coefficients of the diffusing species and the thermodynamic properties of the crystallizing phase.

Refractive index control is essential to prevent transmission losses due to poor waveguiding characteristics. The index difference Δn desired between the core and the cladding of the fibre is typically such that $\Delta n/n \sim 0.01$ [11]. This is achieved by slightly modifying the mole fraction of glass constituants, e.g., PbF_2 raises the index whereas LiF, NaF and AlF_3 lower the index. However, the possibilities of index adjustment procured by composition changes are generally limited by simultaneous degradations of glass thermal stability.

.../...

Transmission losses in optical fibres have extrinsic and intrinsic origins. Intrinsic loss minimum is determined by the $1/\lambda^4$ wavelength (λ)-dependent Rayleigh scattering loss at shorter wavelengths and the multiphonon vibrational absorption edge at longer wavelengths, fig. 5. The position of the multiphonon edge depends to a first approximation on the atomic weight of the anions and cations which form the material, i.e. on the material composition.

- Extrinsic losses are due to light scatterers, classified in three recognized groups, namely : fluoride microcrystallites, oxide particles and voids and impurity absorption bands.

- Light scatterers appear to be predominantly oxide crystallites which may originate from several sources e.g., hydroxides and oxides contained in the raw materials, reaction with H_2O in the synthesis atmosphere, and contamination by container walls or ambient atmosphere.

- Extrinsic absorption losses in the 2-4 µm region, where HMFG-based glasses have their low-loss window, are mainly associated with transition metals, rare earth impurities and OH groups.

The OH fondamental vibration absorption appears at 2.8-2.9 µm. Table 5 after Ohishi et al. gives impurity levels (ppb) causing 0.01 dB/km at different operational wavelength's [14]. At the 2.55 µm wavelength, which emerges as the best compromise for fluoride fibres, it clearly appears that the acceptable impurity contents are extremely low and eventually not compatible with current melt processing. The CVD-route for the preparation of preforms as operated for silica fibres would not be applicable here because of a lack of gas precursors.

On the basis of this presentation, the elaboration of halide optical fibres with a goal of 0.01 dB/km at 2.55 µm is confronted with severe problems which relate to the critical cooling rate, q_c, the material chemical purity and the elaboration process.

.../...

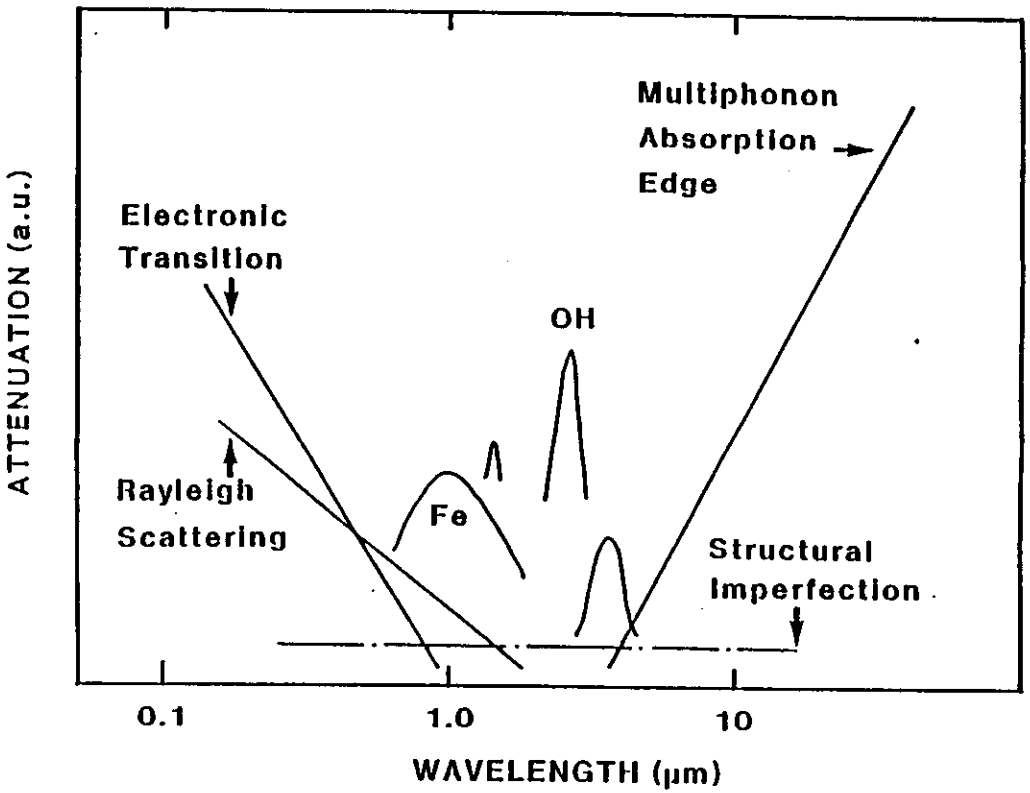

FIGURE 5

Schematic optical attenuation mechanisms in fibres

TABLE 5

Impurity levels (ppb) causing 0.01 dB/km loss at 2.5 μm

IMPURITY	CONTENT
Fe	0.35
Co	0.32
Ni	1.67
Cu	71.50
Nd	1.67
Ce	0.50
Pr	5.55
Sm	3.85
Tb	3.85

The emphasis has been made on halide glasses for the achievement of ultra low-loss fibres. To day indeed, this family is perceived as the most promising alternative to the silica-based family, if the specific difficulties encountered for the achievement of the intrinsic Rayleigh scattering loss can be overcome. However, it must be realized that non-halide routes to obtaining ultra low-loss fibres may emerge in the future. Recently, M.E. Lines has suggested a non-halide route based on the reasoning summarized below [15]. The author observes that intrinsic material low-loss limits in optical fibres are primarily set by Rayleigh scattering losses from frozen-in density fluctuations. The theoretical expression for this loss is proportional to $\ell^2 (d\varepsilon/d\ell)^2$, where ℓ is density and ε the dielectric constant at optical frequencies. It therefore is controlled by the degree to which density fluctuations perturb the dielectric constant. A small increment in density is two-fold. Firstly, it increases the number of bonds per unit volume which in turn increases ε if individual bond contributions are unaffected. Secondly, it may alter the various bond lengths and thereby perturb the chemical nature and affect the polarizability values of individual bonds. The latter perturbation may decrease ε so that a possibility of cancellation exists. If, according to M.E. Lines, Λ is the ratio of the magnitude of the two opposing contributions, then a factor $(1 - \Lambda)^2$ is contained in the density fluctuation contribution to Rayleigh scattering. The author has established that the materials for which a substantial cancellation was most likely were multi-component oxide glasses, especially in the calcium aluminate compositions. On the basis of this theoretical study, a minimum attenuation of around 0.01 dB/km at λ_{min} = 1.9 µm has been predicted for this glass family. This model still has to be validated by experiment. Nevertheless, this example illustrates the fact that the potential of advanced glasses to meet technical requirements is enormous and far from being assessed. It also shows that long-term predictions on the orientations in advanced glass technology may be hazardous.

LIST OF REFERENCES

[1] R.A. Happe, J. of Non-Cryst. Sol. 3 (1970), 375-392.

[2] L.E. Topol & R.A. Happe, J. of Non-Cryst. Sol. 15 (1974), 116-124.

[3] J.P. Coutures, J.C. Riflet, D. Billard & P. Coutures, in : 6th European Symposium on Material Sciences under Microgravity Conditions, Bordeaux (1986), ESA SP-256, p. 427.

[4] M.J. Weber, J. of Non-Cryst. Sol. 42 (1980), 189-196.

[5] O. Deutschbein, M. Faulstick, W. Jahn, G. Krolla and N. Neuroth, Applied Optics 17-4 (1978), 2228-2232.

[6] S.E. Stokowski, W.E. Martin and S.M. Yarema, J. of Non-Cryst. Sol. 40 (1980), 481-487.

[7] W. Huang, C.S. Ray & O.E. Day, J. of Non-Cryst. Sol. 86 (1986), 204-212.

[8] M.J. Weber, D. Milam and W.L. Smith, Optical Engineering 17-5 (1978), 463-469.

[9] G. Neilson and M.C. Weinberg, J. of Non-Cryst. Sol. 23 (1977), 43-58.

[10] M. Poulain, J. Lucas and P. Brun, Mat. Res. Bull. 10 (1975), 243.

[11] S. Sakaguchi & S. Takahashi, J. of Lightwave Technology, V. LT-5, N9 (1987), 1219-1227.

[12] N.P. Bansal, A.J. bruce, R.H. Doremus & C.T. Moynihan, J. of Non-Cryst. Sol. 70 (1985), 379-396.

[13] T. Kanamori, in : Proc. IV Int. Conf. Halide Glasses (Montery, CA), Jan. 26-29, 1987.

[14] Y. Ohishi, S. Mitachi, T. Kanamora & T. Manabe, Phys. Chem. Glasses 24 (1983), 135-140.

[15] M.E. Lines, J. of Non-Cryst. Sol. 103 (1988), 2796288.

FIGURE CAPTIONS

1 - Refractive index versus Abbe numbers for oxides. The enclosed area relates to commercial glasses, after ref. 1.

2 - Schematic of a partial dispersion versus Abbe number for borate, silicate and phosphate glasses, after ref. 1.

3 - Known regions of refractive index and reciprocal dispersion (Abbe number) of optical glasses. Lines of constant Υ at long wavelengths have been estimated from equations 5a-b, after ref. 8.

4 - Intrinsic optical attenuation of various glass families, after T. Manabe.

5 - Schematic optical attenuation mechanisms in fibres.

TABLE CAPTIONS

1 - Some major glass families.

2 - Optical properties of some oxides, after a bibliographic study of P.A. Happe [1].

3 - Non-linear refractive index coefficients of glasses measured interferometrically using linearly polarized 1064 nm laser pulses, after a bibliographic study of M.J. Weber et al., ref. 8.

4 - Critical cooling rates q_c for typical fluoride glasses.

5 - Impurity levels (ppb) causing 0.01 dB/km at 2.5 μm.

IV - STATE OF THE ART IN GPS

IV.1 - General remarks

A paradoxical situation, typical of MPS activities conducted thus far, is that even though few glass experiments were made in space, their goals as well as the materials investigated were extremely diverse. Complementary weightlessness experiments involving other sources of microgravity - e.g., aircraft parabolic flights and drop-tubes have completed past space experiments. Thus, the Government Industrial Research Institute (G.I.R.I.) in Japan has tested the melting of glass spheres typically less than one centimeter in diameter in its acoustic levitation furnace onboard a Mitsubishi jet which provided 20 s of low gravity in parabolic flight [1]. Similarly, the M.F.S.C. drop-tube (32 m) has been used by several U.S. teams in order to investigate on the glass forming ability of various systems or to prepare experiments on board STS [2].

Supporting ground-based studies have also been conducted in order to assess the technical viability of GPS on the basis of experimental and theoretical approaches. A non-exhaustive list of all these activities is given in tables 1 and 2 and in a separate set of references A-1 to A-71, classified in ground-based activities, sounding rocket and space experiments.

The diversity of the materials processed in weightlessness clearly appears in these tables. They are listed below :

- Ga_2O_3-CaO-SiO_2, Na_2O-B_2O_3, Ga_2O_3-CaO and PbO-SiO_2 [3,4]
- Na_2O-SiO_2, Rb_2O-SiO_2 [5,6]
- Li_2O-SiO_2, Na_2O-B_2O_3-SiO_2 [7]
- Sc_2O_3, Y_2O_3, Sm_2O_3, Ga_2O_3, Yb_2O_3, La_2O_3,... [8]
- Fluorides [9]
- Chalcogenides Si-As-Te, Ge-Sb-S [10,11]
- Pd Si Cu [2]

.../...

Goals attached to these experiments are equally diverse, e.g. :

- Search for enhanced glass forming ability and new glasses [8,11]
- Analysis of intrinsic properties of new optical glass materials [1]
- Acquisition of basic data, e.g., diffusion coefficients and thermocapillary characteristics [7] [12]
- Study of actual and model glass shells for I.C.F. [13]
- Investigations on bubble behaviour [14]
- Operational check of instrumentation, e.g. furnace, positioning equipments, etc... [3]

Ground based studies have addressed basic difficulties which may conceptually be anticipated in GPS regarding mainly, precursor materials and glass fining, as well as i) experimental investigations on the glass-forming ability of particular oxides and ii) technical works on new levitation techniques.

The absence of extended and coherent programmes on the one hand and frequent instrumental failures - not to mention crashes upon recovery, e.g., SPAR 8 flight - do not allow an unambiguous evaluation of the benefits drawn from past space experiments. Furthermore, little information is available regarding the characterization of space-made samples.

Nevertheless, some useful indications can be derived from both past space and ground-based experiments. They are briefly discussed in the following within the scope of :

1/ Contemplated benefits from GPS, namely :
- The extension of vitrification domains to difficult glass formers in bulk shape.
- The access to glass intrinsic physical properties and thermodynamical data.
- Space-adapted processes.

2/ Technological steps necessary in order to successfully achieve GPS experiments, namely :
- Preparation of precursor materials and composition homogeneization.
- Glass fining.

.../...

IV.2 - Experimental evidence of the benefits expected from GPS

IV.2.1. Extension of vitrification domains

Glass forming tendency is related to mechanisms and parameters which prevent the occurrence of liquid-solid transformation. It is severely inhibited by heterogeneous nucleation as it was shown in chapter 2. Containerless processing in a weigthlessness environment by suppressing container walls, eliminates a major source of heterogeneous nucleation. The contemplated extension of vitrification domains through GPS primarily stems from this property.

The most significant results which relate to a possible extension of vitrification domains actually follow from free-fall and levitation experiments conducted on the ground.

Laser-spin melting and free-fall cooling experiments have produced new lanthanide oxide glasses, interesting for their optical properties, which could be evaluated [8]. Drop-tube experiments (MFSC, 32 m) have produced bulk glass spheres of $Pd_{77.5}Si_{16.5}Cu_6$, 1.5 mm in diameter, which turned out to be more stable than those produced in water-quench experiments. This was established from the measurement of the temperature interval, $\Delta T = Tc - Tg$: drop-tube samples had ΔT values of around 48 K against 10 to 40 K for water-quenched samples. Furthermore, no sign of crystal nucleation was observed neither on the surface nor in the interior of the sphere at an average cooling rate of 5×10^2 $K.s^{-1}$ (the predicted critical cooling rate using available TTT curves was $\sim 10^2$ $K.s^{-1}$).

A limitation of free fall experiments, which may provide excellent low-g levels, is the duration of free fall ($\sim$2.6 s in the above example). This sets severe limits on the sample size especially for low-melting systems, cooling occurring by radiation only (It is worth noting here the development of a drop-tower in Japan which should allow a free-fall duration of 18 s).

.../...

Aerodynamic levitation experiments performed in a wind-tunnel [15] or on a gas film [16] have also produced interesting results. Thus, glassy materials have been obtained from Y_2O_3, $Y_3Al_5O_{12}$ and recently $Bi_2Sr_2Ca_1Cu_2O_x$ [17]. Such experiments actually suppress the contact with solid container walls but the interaction with the sustaining gas is not negligible and may explain surface crystallization frequently observed in levitated samples.

Therefore, it can be claimed that GPS has a potential for the extension of vitrification domains even though this has not been directly demonstrated in past space experiments because of technical failures.

IV.2.2. Access to glass intrinsic physical properties and to thermodynamical data

GPS offers unique possibilities for the acquisition of intrinsic physical properties by providing reference samples and for the acquisition of basic thermodynamical data by providing experimental conditions - absence of hydrostatic pressure - not accessible on Earth.

The potential for the preparation of reference samples stems from the possibility to process large liquid volumes without containers. Direct contemplated benefits include i) the preparation of high-purity materials, a necessity for instance in the case of halide glasses aimed at optical telecommunications, for which impurity levels must not exceed the ppb level, ii) the elimination of heterogeneous nucleation, with in turn the probable extension of the range of vitrification to new compositions, e.g., high-melting, highly corrosive glass forming melts or compositions highly sensitive to heterogeneous nucleation, and iii) the preparation of homogeneous glasses due to the absence of sedimentation.

Reference samples are essential to the physicist to evaluate the intrinsic properties of the materials. This is the case for instance of the non-linear index, n_2, and the spectroscopic properties of Nd^{3+} ions for glass lasers [18] and of the hydrostatic photoelastic (or Pockels') coefficient for the assessment of ultra-low Rayleigh scattering losses in optical fibres [19]. Indeed, there are no theoretical models able to predict these quantities from the sole knowledge of the compound chemical composition.

.../...

GPS activities in this area will mainly be research-oriented. They will have a direct impact on technology by contributing to the selection of the most performing advanced materials. It must be realized that GPS will be necessary - as opposed to ground-based microgravity sources - in many instances for simple reasons of sample size, cooling duration, etc... Keeping in mind the example of optical fibres for telecommunications, the evaluation of the extremely low attenuations envisaged will require fibres typically 200 m in length i.e. shaped glass samples about 10 cm^3 in size ; this cannot be achieved by non orbiting-means. So far, the area of reference samples made in the microgravity environment has not been investigated.

Basic thermodynamical data are crucial in order to develop quantitative models of glass transformation kinetics and to derive the TTT curves, essential items in process control. Two types of data are required, one of which can be readily evaluated by conventional techniques on the ground, e.g., the free energies of formation $\Delta Gn^*(T)$ and surface tension $\sigma(T)$ (refer to general expressions 15a, b, c of nucleation rate, chapter 2). On the contrary, data on diffusion mechanisms cannot be obtained in the liquid state on the ground. This lack of the latter data is at the origin of unacceptable uncertainties on the critical cooling rate, q_c, of most glass systems as discussed in chapter 2-5. Pionneering experiments of G-H-Frischat et al. on board TEXUS sounding rockets and STS flights have already shown that diffusion data could be obtained with a high accuracy in the microgravity environment (5, 6, 7, 20). Such studies should result in a better control of glass formation on the ground.

IV.2.3. Space-adapted processes

The space environment offers unique properties in terms of processes which may have a dramatic impact on advanced technology as this has been the case in the past with the emergence of new elaboration processes, e.g., the CZOCHRALSKI process for single crystals and chemical vapour deposition (C.V.D.) for semiconductors and silica fibres. However, this aspect of GPS has generally been ignored thus far but for one interesting exception : the achievement of perfect glass shells as thermonuclear fusion targets.

.../...

The production of these targets is a critical path item in the I.C.F. programme for the following reasons as developed by R.L. Down et al. [13]. I.C.F. targets are spherical glass shells (current glasses or metallic glasses) filled with deuterium-tritium fuel. Shells have currently diameters between 0.1 and 1 µm and wall thicknesses from 0.5 to 10 µm. Geometrical requirements are severe, i.e. typically :

- non-concentricity of the inner and outer surfaces of the shells better than 1 %,
- asphericity less than 1 %,
- surface irregularities less than 0.5 µm in magnitude.

These specifications become even more stringent as the size of the sphere increases to a few millimeters, i.e. well above the effective size limit of about 1 mm for conventional fabrication methods [21 to 23].

One of these fabrication methods involves the use of metal-organic powder, which is fed into an electrically-heated vertical tube furnace whereby glass is formed. Metal-organic gels as glass precursors permit the formation of hollow glass spheres with a broad variety of glass composition.

For large glass shells ($\emptyset$ > 1 mm), required for future I.C.F. programmes, gravity and aerodynamic forces act out upon the falling molten shells and degrade both their concentricity and sphericity. In addition, free-fall conditions severely limit the glass fining interval in this process. Therefore, the preparation of bubbles for I.C.F. in a weightlessness environment appears to be a promising alternative to earth-based manufacture of large-diameter perfect shells. The basic idea here is to form perfect spheres under the influence of undisturbed surface forces.

The USA have supported a vigorous and sustained programme on the elaboration of glass shells in weightlessness. NASA has initiated a 3-year contract (1978-1981) aimed at i) understanding the mechanisms which control the formation of highly uniform glass shells suitable for I.C.F., and ii) evaluating the means necessary to make large shells in space [13]. This study was conducted with the gel approach described above.

.../...

Simultaneously, JPL investigated the formation of shells made of metallic glasses of high-atomic number, e.g., the alloy $Au_{55}Pb_{22,5}Sb_{22,5}$ by a free-fall technique. Perfect spheres 1.5 mm in diameter were produced by this method [24].

These programmes were later completed by microgravity experiments in KC-135 parabolic loops, on board SPAR sounding rockets 7-8 [25] and on board STS-61 A(D1). The SPAR 8 experiment was dedicated to model experiments aimed at the study of 3 aspects of the processing of rigid shells in space : drop sphericity, bubble centering and adiabatic bubble expansion. Shells were composed of water and air (5.8 and 4.2 cm^3 respectively). The positioning equipment was a triaxial acoustic resonance chamber. This experiment was rather successful. The sphericity of the outer shell was better than 1 % during the periods when it was not manipulated by the acoustic field. However, the concentricity could not be assessed because of the presence of parasite small bubbles.

The experiment on board STS-61 A(D1) conducted in the MEA/A-2 [3] was aimed at a feasibility study of the reshaping of a large glass shell. A soda-lime-silica glass shell containing an air bubble ~3.75 mm in diameter was used for this purpose. The experiment failed because of a malfunction of the positioning equipment.

This programme of the formation of glass shells in microgravity is examplary in that it is a multidisciplinary programme which relates to a long-term major energy programme. Obviously, few other programmes could have benefitted from the same support and survived the long delays due to repeated failures and to the lack of flight opportunities.

IV.3. Experimental evidence on Technical Aspects of GPS

IV.3.1. Precursor materials and sample homogenization

The availability of precursor materials and the homogenization of complex compounds are two important items in glass technology where the glass formation protocol requires a melting step.

On earth, the melting step naturally occurs in a crucible, precursors materials may be pressed powders or solid blocks and the homogenization of the melt is currently achieved either by gravity-driven convection or by mechanical stirring.

Containerless processing in space raises the problem of the homogenization of the melt at the macroscopic and microscopic levels, especially in the case of multicomponent glasses which are precisely the most promising ones for future applications.

Various solutions have been envisaged in order to overcome these problems - and eventually the fining of the glass discussed below - which involve the development of either specific processes in space - e.g. stirred liquid bridges - or precursor materials which guarantee ultra-pure, chemically homogeneous starting materials.

An important study has been made in the latter direction by S.P. Mukherjee from Battelle [26]. This study aimed at the development of ultrapure optical waveguides in microgravity envisaged the fabrication of sol-gel precursors for silica-based glasses. The sol-gel process was based on the polymerization reaction of alkoxysilane with other metal-alkoxy compounds. Another ground-based research study on gel precursors as glass ceramic starting materials for space processing was conducted on tungstate glasses interesting for their

optical properties [27]. The advantages of the sol-gel approach are generally three-fold namely :

. it provides ultra-pure starting materials,
. it involves relatively low-temperature processes [28],
. it gives the structural skeleton of the glass network and in turn the material chemical homogeneity.

Unifortunately this approach well-suited for oxide glasses [29] is not universal. Moreover, it has not been qualified in space experiments thus far. Therefore, precursor materials and glass homogenization are still unsolved problems for GPS.

IV.3.2. Glass fining

The formation of a glass requires at one stage or another the melting of raw materials. This melting steps liberates gases which are chemically combined - e.g., CO_2 in oxide glasses prepared from carbonate starting materials - or included in the raw materials, e.g. adsorbed and intergranular gases in pressed starting materials. In all cases, this leads to bubble entrapment in the glass. This phenomenon has been advantageously exploited in several applications but in most cases it has a redhibitory effect. Therefore, bubbles must be eliminated in some ways by a so-called fining step.

Three fining principles, which eventually cooporate, are currently used, namely [25] :

. buoyant fining,
. chemical fining,
. thermal fining.

Buoyant fining is the simplest fining mechanism on earth. It occurs as a result of buoyant forces which push the bubbles upwards out of the melt at a velocity v approximately given by,

$$v = D^2 g \rho / 12\eta \qquad (1)$$

where D is the bubble diameter, g is the acceleration of gravity, ρ is the density of the glass and η is the viscosity of the glass. Nevertheless, this mecanism is not sufficient to explain the fining of commercial glasses, e.g. a bubble 10µm in diameter in a 100 poise fluoride melt would rise at a velocity of around 0.3 cm/day !

Chemical fining is another process widely used in industry and involving complex microscopic mechanisms which have not been fully understood so far [30, 31]. Chemical fining is based on the use of additives, e.g. arsenic and antimony oxides, in small concentration, which in some cases at least favour the formation of large bubbles easily eliminated by buoyant forces.

The first process and the second one to some extent are effective in the presence of the gravity yield. They are no more operative in the microgravity environment.

A third fining process, referred to as thermal fining, is independent of the gravity field. Its principle relies on the fact that bubbles are driven by Marangoni forces that cause them to move in a temperature gradient.

Young, Goldstein and Block [32] developed a simple expression for the velocity v of a spherical bubble placed in a temperature gradient in the absence of gravity,

$$v = \frac{dT}{dx} \left(\frac{d\sigma}{dT}\right) D/2\eta \qquad (2)$$

where dT/dx is the temperature gradient, $d\sigma/dT$ is the temperature coefficient of the surface tension of the glass, D is the bubble diameter and η is viscosity. According to this simple expression v is proportional to the temperature gradient - an adjustable parameter - and to the term $d\sigma/dT$, which depends on the glass-gas system. The direction of motion depends on the sign of $d\sigma/dT$ generally negative.

For current values of $d\sigma/dT \simeq -0.15$ dyne/cm°C and $\eta \simeq 100$ poises, typical of fluoride melts, a bubble 10µm in diameter would reach velocity values above 10 cm/day in a temperature gradient of a few 100°C/cm ; these velocities are one to two orders of magnitude larger than those obtained under the influence of buoyancy forces on earth for the same bubble diameter. A more complete treatment of the motion of a bubble under the action of Marangoni forces has been proposed by Subramanian [33].

Clearly, this fining mechanism is most attractive for the formation of glasses under containerless melting conditions in a weightlessness environment. This does not mean that specific fining configurations, e.g. involving stirred liquid bridges, cannot be developed in space which would simultaneously take advantage of the three fining processes.

Thermal fining has been recognized as most important for GPS in the U.S.A. which have dedicated a substantial programme to this topic. This programme was initiated with theoretical investigations and ground-based experiments aimed at supporting microgravity experiments [34]. A non-exhaustive literature on microgravity-related glass fining activities is given in refs [3, 25, 34].

U.S. teams have tentatively flown microgravity experiments aimed at acquiring quantitative date on bubble behaviour in a temperature gradient, e.g. velocity, dissolution or growth, nucleation and coalescence. A borax composition - 33.3 Na_2O - 66.7 B_2O_3 was selected for these experiments and spheres containing

bubbles were prepared on earth by a free fall technique [4]. Samples were flown on board SPAR VIII sounding rocket (Nov. 1980) and twice on board STS-7 and STS 61A (D_1) using the MEA facility.

SPAR VIII experiment alone could be qualitatively exploited. Results obtained were generally consistant with the current model of thermocapillary bubble migration. However, D. Neuhaus & B. Feuerbacher showed in a simulation experiment conducted with several grades of silicon oil on board STS-61A(D_1) that Marangoni forces alone could not fully account for the observed motion of bubbles. They found that an additional dissipative mechanism at the liquid/gas interface was necessary and they suggested "dilational surface viscosity" as the additional parameter. This parameter simply relates to the fact that the surface area of the bubble varies with surface tension σ [12].

Thus, despite significant efforts, mechanisms involved in thermocapillary bubble migration have not been elucidated and a fining protocol in weightlessness still has to be conceived. Furthermore, accurate data on the σ (T) relationship for the different glass-gas system, indispensable for thermal fining, are seldom available.

TABLE 1

EXAMPLES OF GROUND-BASED EXPERIMENTS

N°	SYSTEM	MEANS	ORIGIN	GENERAL GOALS	REFS
1	$Pd_{77,5}$ $Si_{16,5}$ Cu_6	drop tube 32 m (MSFC)	USA	glass shell formation, model for I.C.F. shell	A-38
2	Na_2O-SiO_2	sol-gel precursors	USA	glass shell manufacturing in space for I.C.F.	
3	Lanthanide oxide glasses	laser spin and free-fall cooling	USA	containerless formation of new optical glasses for properties evaluation	A-47
4	Model systems	-	USA	bubble behaviour (thermocapillary driven motion, dissolution, coalescence, etc...) for I.C.F. and glass fining	A-44
5	-	sol-gel precursors	USA	starting materials for space processing	A-16
6	$Y_3Al_5O_{12}$, BiSrCaCuO	aerodynamic levitation and CO_2 heating	FRANCE	containerless formation of new glass materials	A-17
7	Fluoride glasses	levitation on a thin gas film	FRANCE	containerless formation of fluoride glasses and I.R. attenuation analysis	CGE priv.com.

TABLE 2

NON-EXHAUSTIVE LIST OF GLASS EXPERIMENTS CONDUCTED ON-BOARD SOUNDING ROCKETS AND ORBITING SPACESHIPS

SOUNDING ROCKET EXPERIMENTS

N°	GLASS SYSTEM	FLIGHT	ORIGIN	DATE	GOALS	REFS.
1	Na_2O, $3SiO_2$ - Rb_2O, $3SiO_2$	TEXUS 1	F.R.G.	10/77	Interdiffusion coefficient	A-56
2	Ga_2O_3-CaO-SiO_2 (39.3, 35.7, 25 mole %)	SPAR 6	USA	-	Glass formation experiment	A-49
3	Ga_2O_3-CaO-SiO_2 (39.3, 35.7, 25 mole %)	SPAR 8	USA	11/80	Ibidem	A-53
4	Na_2O-B_2O_3	SPAR 8	USA	11/80	Glass fining experiment	A-53
5	Air-water model drops	SPAR 8	USA	11/80	Containerless processing of rigid glass shells for I.C.F.[1]	A-53
6	Alakali-silicate glass	TEXUS 4	F.R.G.	5/81	Corrosion experiment	A-70
7	Alakali-silicate glass	TEXUS 6	F.R.G.	5/82	Self diffusion coefficient	A-58
8	Chalcogenide SiAsTe	TT500, 8	Japan	-	SiAsTe amorphous semiconductor	A-64
9	Chalcogenide SiAsTe	TT550, 13	Japan	8/83	SiAsTe amorphous	A-64
10	B_2O_3-PbO, C composite	TT500, 13	Japan	8/83	Diamond glass composite (model)	A-51-52
11	Na_2O, $3SiO_2$ - Rb_2O, $3SiO_2$	TEXUS 11, 12	F.R.G.	5-6/85	Interdiffusion coefficient	13
12	Na_2O, $3SiO_2$ - Rb_2O, $3SiO_2$	TEXUS 13	F.R.G.	4/86	Interdiffusion coefficient	13
13	Na_2O, $3SiO_2$ - Rb_2O, $3SiO_2$ (?)	TEXUS 19	F.R.G.	11/88	Interdiffusion coefficient and electrostatic levitator test	not available

.../...

TABLE 2 (continued)

SPACE EXPERIMENTS

N°	GLASS SYSTEM	FLIGHT	ORIGIN	DATE	GOALS	REFS
1	Ge_{25} Sb_{20} S_{55}	Soyuz-Salyut	USSR Tech.	1981	Glass formation in a crucible	A-42
2	Ga_2O_3-CaO-SiO_2 (39,3, 35.7, 25 mole %)	STS-7 (MEA/A-1)[2]	USA	11/83	Glass formation and operational check of SAAL[3]	A-45
3	Bi_2 $(TeSe)_3$	Salyut 6	USSR	1983	Glass formation	A-56
4	Ga_2O_3-CaO (56-44 mole %)	STS-7 MEA/A-1	USA	11/83	Operational check of SAAL	A-45
5	Na_2O-B_2O_3 (33.3, 66.7 mole %)	STS-7 MEA/A-1	USA	11/83	Bubble behaviour (motion, dissolution, coalescence)	A-45
6	Na_2O-SiO_2 (45-55 mole %)	STS-7 MEA/A-1	USA	11/83	Glass formation	A-45
7	Soda-lime-silica	STS-7	F.R.G.	11/83	Corrosion	A-60
8	B_2O_3-Pb-C composite	STS-41G (Gas)	Japan	10/84	Diamond glass composite	A-51-52
9	Soda-line-glass	STS-11 (Maus)	F.R.G.	2/84	Bubble behaviour	A-59-71
10	BeF_2-based glasses A-56	Salyut 6	USSR	1984	Bubble formation and motion	
11	Ga_2O_3-CaO-SiO_2 (39.3, 35.7, 25 mole %)	STS-61 A (D1) MEA/A-2	USA	10/85	Enhanced glass formation	A-43
12	PbO-SiO_2	STS-61 A (D1) MEA/A-2	USA		Glass homogeneity and precursor preparation	A-43

---/---

TABLE 2 (continued)

SPACE EXPERIMENTS

N°	GLASS SYSTEM	FLIGHT	ORIGIN	DATE	GOALS	REFS
13	Ga_2O_3-CaO (56-44 mole %)	Ibidem	Ibid.	Ibid.	Enhanced glass formation and properties analysis	A-43
14	Li_2O-SiO_2 and Na_2O-Bi_2O_3-SiO_2	STS-61 A (D1)	F.R.G.	10/85	Glass homogeneity	A-62
15	Ga_2O_3-CaO-GeO_2	STS-FMPT[4]	Japan	1991	Glass formation and I.R. attenuation analysis	A-29
16	ZrF_4, BaF_2, LaF_3 (62-33-5 mole %)	STS	USA	1986	Glass formation and test of 3-axis acoustic levitator	A-67
17	Silicon oil (model)	STS-61 A (D1)	F.R.G.	10/85	Bubble motion in a temperature gradient	A-61
18	Soda-line-silica	STS-61 A(D1)	USA	10/85	Glass shell	A-43
19	33,3 Na_2O - 66,7 B_2O_3	STS-61 A(D1)	USA	10/85	Bubble behaviour	A-43

TABLES 1-3 : LIST OF ACRONYMS

1 I.C.F. : Inertial Confinement Fusion

2 M.E.A. : Material Experiment Assembly

3 S.A.A.L. : Single Acoustic Levitator

4 F.M.P.T. : First Material Processing Test.

LIST OF REFERENCES

1. *J. Hayakawa, M. Makihara, M. Nogami, T. Komiyama et Y. Moriya,*
Proc. 6th European Symposium on Material Science under microgravity conditions,
2-5 Dec. 1986 Bordeaux, ESASP-256, 263-267.

2 *J. Steinberg, A.E. Lord Jr., L.L. Lacy, J. Johnson*
Appl. Phys. Lett. 38-3 (1981) 135-137

3 *D.E. Day & C.S. Ray,*
Final Report for MEA/A-1 experiment 81FO1 conducted on STS7 flight, June 1983, contract NAS-8-34758, containerless processing of glass forming melts - 10 April 1984

4. *D.E. Day & C.S. Ray,*
Final Report for D_1, MEA/A-2 experiment 81FO1 conducted on STS-61A flight, october 1985, Contract NAS-8-34758, containerless processing of glass forming melts - 1 November 1986.

5. *W. Beier, M. Braedt & G.H. Frischat,*
Physics & Chemistry of Glasses, 24-1 (1983) 1-4.

6. *M. Braedt & G.H. Frischat,*
Comm. of the Am. Ceram. Soc., C-54-56, April 1984, 54-56.

7. *V. Braetsch & G.H. Frischat,*
6th European Symposium on Material Science under microgravity conditions, 2-5 Dec. 1986, Bordeaux, ESA SP-256, 259-262.

8. *L.E. Topol, D.H. Hengstenberg & M. Blander,* J. of Non-Crystal Solids 12 (1973) 377-390 and
L.E. Topol and R.A. Happe, J. of Non-Crystal Solids 15 (1974) 116-124.

9. *R.H. Doremus,* NASA-Techn. Memorandum 87568, project N86-10149 for STS-11 flight.

10. *Y. Hamakawa, H. Okamoto & C. Sada*
2nd Japan-Germany - ESA Joint Symposium for material processing in space, March 25-26, 1985, 1 - 14.

11. *C. Barta, J. Trnka, A. Triska & M. Frumar,*
Adv. Space Res. 1 (1981) 121 - 124.

12. *H.D. Smith, D.M. Mattox, W.R. Wilcox, R.S. Subramanian, M. Meyyappan,*
Materials processing in the reduced gravity environment of space, ed. G.E. Rindone (Elsevier Science Publi. Comp. In., 1982) 270-289.

13. *R.L. Downs, M.A. Ebner & R.L. Nolen,*
Final Report, glass shell manufacturing in space, 21 Dec. 1981, NAS8 - 33103.

14. *D. Neuhaus & B. Feuerbacher*
Scientific Results of the German Spacelab Mission D1,
Norderney Symposium 27-29 August 1986, eds P.R. Sahm, R. Jansen, M.H. Keller ISBN3-89100-013-8, 118-121.

15. *P.C. Nordine & R.M. Atkins,*
Rev. Sci. Instrum., 53 (9) (1982) - 1456 - 1464.

16. *J. Granier & C. Potard,*
8th Int. Conf. on Crystal Growth (ICCG-8), York 13-18 July 1986.

17. *J.P. Coutures,* Private Communication, 1988.

18. *M.J. Weber, D. Milam & W.L. Smith,*
Opt. Eng. 17-55 (1978) 463-469

19. *M.J. Weber,*
J. of non Cryst. Sol. 42 (1980) 189-196

20. *K. Herr, H.J. Barklage, Higefort & G.H. Frischat*
Proc. 3rd European Symposium on Material Science in Space
24-27 April 1979, Grenoble, ESA-SP142.

21. *F. Veatch, H.E. Alford & R.D. Croft,*
Hollow glass particles & methods of producing same
U.S. patent Nb. 3, 030, 125, April 17, 1962.

22. *W.R. Beck & D.L. O'Brien,*
U.S. Patent n° 3, 365, 315, April 23, 1968.

23. *C.D. Hendricks,* U.S. patent n° 4, 163, 637, August 7, 1979.

24. *M.C. Lee & J.M. Kendall*
Advances in Ceramics, 19855N 0730 - 9546,
V5 Materials processing in space
Ed. B.J. Dunbar, the Am. Ceram. Soc, (1983), 178 - 185.

25. *R.P. Chassay & E.G. Osburn,* NASA Techn. - Memorandum 82578.

26. *S.P. Mukkerjee, J.C. Debsikdar & T.L. Beam,*
Final Report NASA-CR-169939 - 31 July 1981 (NAS7-100).

27 *R.L. Downs & W.J. Miller,*
Annual Report, 13 Dec. 1982 - 13 Dec. 1983, NASA-CR-176113.

28 *M. Yamane, S. Inoue & K. Nakazawa,*
J. of Non Cryst. Sol. 48 (1982) 153-159.

29. *V. Gottardi,* ed., Glasses and glass ceramics from gels,
Proc. Int. Workshop on glasses and glass ceramics from gels, Padova, (Italy) - October 8-9 1981
J. of Cryst. Sol. 48 (1) , March 1982.

30. *G.H. Greene & R.F. Gaffrey,*
J. Am. Ceram. Soc. 42 - 6 - (1959) - 273.

31. *L. Nemec,*
J. Am. Ceram. Soc., 60-10 (1977) 436-440.

32. *N.O. Young, J.S. Goldstein & M.J. Block,*
J. Fluid. Mech. 6 (1959) 350.

33. *R.S. Subramarian,* AICHE J., Sept. 1980.

34. *W.R. Wilcox, R.S. Subramanian, M. Meyyappan, H.D. Smith, D.M. Mattox & D.P. Partlow,*
Final Report NASA Contract NAS8-33017.

LITERATURE ON GLASS PROCESSING IN SPACE

- References A1 to 71 -

Prospective analysis

[1] ***N.J. Kreidl,*** Glass experiments in space, J. of Non Crystalline Solids 80 (1986) 587-593.

[2] ***N.J. Kreidl & G.E. Rindone,*** Glass in space, J. of Non Crystalline Solids 38 & 39 (980) 825-830.

[3] ***S. Ramaseshan,*** Materials processing in space, a brief revue, Bull. Mater. Sci. 4.2 (1982) 53-73.

[4] ***M. Weinberg,*** Glass processing in space, the glass industry, March 1978, 22-27.

[5] ***P. Ramanchandrarao,*** Processing of ceramics and glasses in space, Bull. Mat. Sci. 4-3 (1982) 261-266.

[6] ***D.C. Larsen,*** Theoretical study of production of unique glasses in space, NASA Contract n° NA58-29850, July 23, 1974.

[7] ***G. Seibert,*** Material sciences in space, ESA Journal, 2 (1978) 99-109.

[8] ***G.F. Neilson & M.C. Weinberg,*** Outer space formation of a laser host glass, J. of Non Crystalline Solids 23 (1977) 43-58.

[9] ***R.A. Happe,*** Manufacturing unique glass in space, Contract NAS8-29881, March 32, 1976.

[10] ***G.F. Neilson & M.C. Weinberg,*** Outer space formation of a laser host glass, J. of Non Crystalline Solids 72 (4977) 43-58.

[11] ***G.F. Neilson & M.C. Weinberg*** Outer space formation of a laser body glass, J. of Non Crystalline Solids 23 (1977) 43-58.

[12] ***M.C. Weinberg, G.F. Neilson & M.A. Zak,*** A feasibility study of the production of low loss IR fibers in space, November 15, 1983.

[13] *J. Zarzycki, B.H. Frischat, D.M. Hetlach,* Glasses in : fluid sciences and materials science in space, ed. H.U. Walter (Springer Verlag, 1987) 599-634.

[14] *D.R. Uhlmann,* Glass processing in a microgravity environment, in : Advances in Ceramics, 5 - Materials processing in space, ed. B.D. Dunbar (Am. Ceram. Soc. Inc., Columbus, Ohio) 118-127.

[15] *C.D. Heindricks,* Materials processing in space : ICF target fabrication implications, Ibid., 132-138.

Ground-based experiments

[16] *R.L. Downs & W.J. Miller,* Research study for "gel precursors as glass and ceramic starting materials for space processing applications research" - NASA 7-100, March 12, 1983.

[17] *M.A. Russak,* Homogeneization of multicomponent glasses, J. of the Am. Ceram. Soc., 61-34 (1978) 181-182.

[18] *R.F. Firestone & S.W. Schramm,* Space processing of chalcogenide glass, Contract n° NAS8-32388, October 31, 1988.

[19] *D.C. Larsen & M.A. Ali,* Space processing of chalcogenide glass, NASA-CR-153001, Sept. 30, 1976.

[20] *R.L. Downs, M.A. Ebner & N.L. Nolen,* Glass shell manufacturing in space, NAS8-33103, December 21, 1981.

[21] *M. Meyyappan & R.S. Subramanian,* The thermocapillary motion of two bubbles oriented arbitrarily relative to a thermal gradient, J. of Colloid & Interface Science, 897-1 (1984) 291-294.

[22] *V. Rosenkranz, V. Braetsch & G.H. Frischat,* Gas bubbles in glass melts under microgravity. Part 1, apparatus for photographic observation, Physics and Chemistry of Glasses, 26-4 (1985) 123-125.

[23] *P. Annamalai, N. Shankar, R. Cole & R.S. Subramanian,* bubble migration inside a liquid drop in a space laboratory, Applied Scientific Res. 38 (1982) 179-186.

[24] *K.A. Happe & K.S. Kim,* Containerless prepartion of advanced optical glasses, Experiment 77F095, NAS8-32953, March 1, 1982.

[25] *R.D. Smith, D.M. Mattox, W.R. Wilcox, R.S. Subramanian & M. Meyyappan,* Experimental observation of the thermocapillary driven motion of bubbles in a molten glass under low gravity conditions, in : Materials Processing in the Reduced Gravity Environment of Space, ed. G.E. Rindone (Elsevier Science Publ. Comp. Inc., 1982) 270-289.

[26] *S.P. Mukherjee,* Gels and gel-derived glasses in the system Na_2O-B_2O_3-SiO_2, in : Advances in Ceramics, 5, Materials Processing in Space, ed. B.J. Dunbar (The Am. Ceram. Soc. Inc., Columbus, Ohio) 91-101.

[27] *M. Meyyappan, R.S. Subramanian, W.R. Wilcox & H. Smith,* Ibidem, 128-131.

[28] *T.J. Mc Neil, R. Cole & R.S. Subramanian,* Surface-driven tension flow in glass melts and model fluids, Ibidem, 167-177, D.M. Herlach, W. Willmeker & F. Gillessen, in : Proc. of the 5th European Symposium on Material Sciences under Microgravity, Schloss Elmau - ESA SP-222 (1984) 389-397.

[29] *J. Hayakawa, M. Makihara, M. Nogami, T. Komiyama & Y. Moriya,* Glass melting test under microgravity produced by aircraft, in : Proc. 6th European Symposium on Materials Sciences under Microgravity Conditions, Bordeaux, ESA SP-256 (1987) 263-267.

[30] *E.C. Etheridge, P.A. Curreri & D. Pline,* Heterogeneous nucleation and glass-formation studies of 56 Ga_2O_3, 44 CaO systems, J. Am. Ceram. Soc. 70 (4987) 553.

[31] *P. Kondo, R.S. Subramanian & M.C. Weinberg,* The dissolution or growth of a gas bubble inside a drop in zero gravity, in MRS Symposia Proc. Materials Processing in the Reduced Gravity Environment of Space, Volume 87 (R.H. Doremus & P.C. Nordine, eds.), MRS, 1987, 261-269.

[32] *J. Mathew & R.H. Doremus,* Outgassing of ZrF_4-based glasses, J. Am. Ceram. Soc. 70 (1987) C-86.

[33] *C.S. Ray & D.E. Day,* Crystallization of 2 Bi_2O_3 - 3 GeO_2 glass in Proc. 15th Annual Meeting of North American Thermal Analysis Society (1986) 353-358.

[34] *C.S. Ray, W. Huang & D.E. Day,* Crystallization of lithia-silica glasses : effects of composition and nucleating agents, J. Am. Ceram. Soc. 70 (1987) 599.

[35] *N. Shankar & R.S. Subramanian,* The stokes motion of a gas bubble due to interfacial tension gradients at low to moderate Marangoni numbers, J. Colloid & Interface Sci. 123 (1988) 512.

[36] *R.S. Subramanian,* The behaviour of multiphase systems in low gravity, in Low Gravity Sciences (J.N. Koster, ed.) AAS, 1987.

[37] *M.C. Weinberg,* A test of the Johnson-Mehl-Avrami equations, J. Cryst. Growth 82 (1987) 779.

[38] *C.S. Kiminami & P.R. Sahm,* Kinetics of crystal nucleation and growth in $Pd_{77.5}$ $Si_{16.5}$ Cu_6 glass, Acta Met. 1986 (in press).

[39] *C.P. Lee & T.G. Wang,* The centuring dynamics of a thin liquid shell in capillary oscillations, J. Fluid Mech., 1988 (in press).

[40] *R.M. Merritt & R.S. Subramanian,* The migration of isolated gas bubbles in a vertical temperature gradient, J. Colloid & Interface Sci., 1988 (in press).

Microgravity experiments

[41] *H.D. Smith, D.M. Mattox, W.R. Wilcox, R.S. Subramanian & M. Meyyappan,* in Materials processing in the reduced gravity environment of space, ed. G.E. Rindone (Elsevier Science Publ. Comp. Inc., 1982) 279-288.

[42] *C. Barta, J. Trnka, A. Triska et M. Frumar,* Recrystallization of glasses of the Ge-Sb-S system prepared under zero gravity conditions, Adv. Space Res. 1 (1981) 121-124.

[43] *D.E. Day & C.S. Ray,* Containerless processing of glass forming melts - D1, MEA/A2 experiment 81 F01 conducted on STS-61 A flight, October 1985, NASA-CR-179118, Nov. 1, 1986.

[44] *W.R. Wilcox, R.S. Subramanian, M. Meyyappan, H.D. Smith, D.M. Mattox, D.P. Partlow,* A preliminary analysis of the data from experiment 77-13 and final report on glass fining experiments in zero gravity, NAS8-33107.

[45] *D.E. Day & C.S. Ray,* Containerless processing of glass forming melts, MEA/A1 experiment 81F01 conducted on STS - 7 flight, june 1983, NASA-CR-171048, April 10, 1984.

[46] *L.E. Topol & R.A. Happe,* formation of new lanthanide oxide glasses by laser spin melting and free-fall cooling, J. of Non Crystalline Solids 15 (1974) 116-124.

[47] *L.E. Topol, D. Hengstenberg, M. Blander, R.A. Happe, N.L. Richardson & L.S. Nelson,* Formation of new oxide glasses by laser spin melting and free-fall cooling, J. of Non Crystalline Solids 12 (1973) 377-390.

[48] *W. Beier, M. Braedt & G.H. Frischat,* Reactions between vitreous silica and sodium silicate glass melts under weightless conditions, physics and chemistry of glasses 24-1 (1983) 1-4.

[49] *C.S. Ray & D.E. Day,* Description of the containerless melting of glass in low gravity, 15th National SAMPE Technical Conference, October 4-6 (1983) 135-145.

[50] *V. Braetsch & G.H. Frischat,* Homogeneity of Li_2O-SiO_2 glasses as prepared under microgravity and 1-g melting conditions, Naturwissinshaften 73 (1986) 368-369.

[51] *T. Noma, J. Tanii, Ryushi Kuwano & A.B. Sawaoka,* Diamond-glass composite processing in a microgravity condition, Jap. J. of Applied Phys. 25-12 (1986) L 955-957.

[52] *T. Noma & A. Sawaoka,* Fabrication of diamond-glass composite under microgravity, Jap. J. of Applied Phys. 24-10 (1985) 1298-1301.

[53] *R.P. Chassay,* Space processing applications Rocket project, spar VIII final report - containerless processing of glass, glass-fining experiment in low-gravity and dynamics of liquid bubbles, NASA - TM 83578, 1984.

[54] *J. Steinberg, A.E. Lord, L.L. Lacy & J. Johnson,* Production of bulk amorphous $Pd_{77,5}$ $Si_{16,5}$ Cu_6 in a containerless low-gravity experiment, Appl. Phys. Lett. 38-3 (1981) 135-137.

[55] *L.R. Regel,* Solidification des verres en microgravité, Sciences des Matériaux dans l'Espace (Technique et Documentation Lavoisier, 1984), 87-94.

[56] *K. Herr, H.J. Barklage-Hilgefort & G.H. Frischat,* Reactions between glass melts, in : Proc. of 3rd European Symp. on Material Sciences in Space, Grenoble, ESA-SP-142 (1979) 263-266.

[57] *G.H. Frischat, M. Braedt & N. Beier,* reactions in glass smelt systems in : Proc. of the 4th European Symp. on Material Sciences under Microgravity, Madrid, ESA-SP-191 (1983) 161-165.

[58] *M. Braedt, V. Braetsch & G.H. Frischat,* Interdiffusion in the glass melt system (Na_2O + Rb_2O) $3SiO_2$, in : Proc. of the 5th European Symposium on Material Sciences under Microgravity, Schloss Elman (ESA-SP-222 (1984) 109-112.

[59] *V. Rosenkranz & G.H. Frischat,* Shrinking of a gas bubble in a glass melt under microgravity conditions, Ibidem, 353-357.

[60] *V. Braetsch & G.H. Frischat,* Influence of microgravity on the homogeneity of glasses, in : Proc. 6th European Symposium on Material Sciences under Microgravity Conditions, Bordeaux, ESA-SP-256 (1987) 259-262.

[61] *D. Neuhaus & B. Feuerbacher,* Bubble motions indiced by temperature gradient, in : Proc. of the Norderney Symposium on Scientific Results of the German Spacelab Mission D1. eds. P.R. Sahm, R. Jansen & M.H. Keller (WPF c/o DFVLR, Köln Germany, 1987) 118-121.

[62] *V. Braedt & G.H. Frischat,* Homogeneity of glasses prepared under microgravity and 1-g melting conditions, Ibidem, 166-171.

[63] *C.S. Ray & D.E. Day,* Glass formation in microgravity, Ibidem, 179-187.

[64] *Y. Hamakawa, H. Okamoto & C. Sada,* Fabrication of Si-As-Te amorphous semiconductor in the microgravity environment in space, in : 2nd Japan-germany - ESA Joint Symposium for Material Processing in Space, March 25-26, 1985, 1-14.

[65] *M.C. Lee & J.M. Kendall,* in : Advances in ceramics vs materials processing in space, ed. B.J. Dunbar, The Am. Ceram. Soc., ISSN 0730-9546 (1983) 178-185.

[66] *M. Braedt & G.H. Frischat,* Com. of the Am. Ceram. Soc. C-54, April 1984, 54-56.

[67] *M. Barnatz,* Orienting acoustically-levitated aspherical objects, NASA Tech. Briefs, NPO 16846, 1988.

[68] *P.A. Bahrami & T.G. Wang,* Analysis of gravity and conduction driven melting in a sphere, J. Heat Transf., 1988 (submitted).

[69] *I.N. Chakraborty, H. Rutz & D.E. Day,* Glass formation, properties and structure of Y_2O_3-Al_2O_3-B_2O_3 system, J. Non-Cryst. Solids 81 (1986) 173.

[70] *H.J. Barklage-Hilgefort, G.H. Frischat,* reactions between SiO_2 and Na_2O-$3SiO_2$ glass melts, Phys. Chem. Glasses 21 (1980) 212-215.

[71] *V. Jeschke & G.H. Frischat,* Gas bubbles in glass melts under microgravity, helium diffusion, Phys. and Chemistry of Glasses 28-5 (1987) 177-182.

V. INDUSTRIAL PERSPECTIVES BOUND TO GLASS PROCESSING IN MICRO-GRAVITY

A number of evaluations of the potential of glass processing in space for applications in industry have appeared in literature, e.g., refs 1 to 4. It is widely accepted in these surveys that the potential of GPS should stem mainly from the possibility to process large melt volumes without containers and to take advantage of space-adapted processes. However, it is hazardous to-day to speculate on specific applications or exploitations of this potential for a number of well-known reasons some of which are briefly mentioned in the following. Firstly, the detailed impact - direct or indirect - of the gravity field on the processing of glasses is generally not understood or eventually ignored by the scientific community. Secondly, the ultimate balance of advantages procured by GPS, either technical or economical, is not clearly perceived in the long-range. In this context, the emergence of competitive ground-based techniques is a permanent possibility to be taken into account and currently opposed by industry to any committment in GPS. Thirdly, the information collected from past space experiments does not provide sound basis for such a committment. Indeed, early GPS experiments dramatically suffered from inevitable limitations due to a combination of insufficient experience in microgravity, low performance of instrumentation, lack of multidisciplinary evaluations, etc...

All these factors have favoured controversial appreciations of GPS - and MPS as well - and skepticism from the scientific community.

Nevertheless, it cannot be ignored that i) the technical potential of GPS has been unveiled in several successful experiments, e.g., measurement of self-diffusion coefficients and demonstration of the possible extension of vitrification domains and ii) R & D on earth has already benefitted from past space experiments. The latter benefits follow from both theoretical investigations and ground-based experiments which were made necessary as a support to space experiments. Thus, basic studies on the dynamics of hollow spheres [5] and on

the phenomena associated with thermomigration [6] have resulted in substantial progress in these areas. Concomittantly, drop-tubes have been increasingly used all over the world in order to perform solidification experiments in weightlessness and to investigate on vitrification domains ; Japan is developing a drop tube which will allow up to 18 seconds in weightlessness. Another fall-out of space experiments is the rapid development of levitation techniques with the aim of suppressing direct contact between liquid and container walls. One of these techniques, based on the gas-bearing principle has a unique potential for the processing of large and shaped volumes on earth [7]. It has been recently implemented in a few laboratories including industrial laboratories for their investigations on ultra-low loss fibres for optical telecommunications [8, 9, 10].

All these studies stimulated by GPS - and MPS in general - contribute to a better understanding of the role of the gravity field in glass processing and to drastic improvements in the preparation of the future space experiments. This emerging cross-fertilization between earth - and space - based experiments may stimulate GPS experiments especially in the following directions :

. Acquisition of the basic data necessary for a quantitative assessment of transformation kinetics (TTT curves). At present this information is missing for virtually all glass systems and in many instances it requires long-duration experiments in weightlessness as discussed in chapter 2.

. Acquisition of basic data on the vitrification domain of border-line or new compositions by suppressing heterogeneous nucleation caused by container walls. This applies to all systems for which drop-tube or rocket experiments are not sufficient in terms of weightlessness duration.

. Acquisition of intrinsic physical data on reference samples typically $1cm^3$ or larger (e.g. 10 cm^3 for ultra-low loss materials) for performance evaluation purposes.

. Acquisition of basic data on the technology of glass processing applicable to earth and space-bound processing, which relate to e.g., thermomigration, fining, homogenization, etc...

. Demonstration of the feasability of space-adapted processes, e.g., regarding hollow spheres, glass-ceramics tailoring, liquid bridges, etc...

As far as long term projections are concerned, some reasons have already been put forward to justify a cautious attitude. Furthermore, it must also be realized that little is known of glass technology at a time when GPS may be fully exploited, i. e. 10 to 20 years from now with the setting in operation of the large orbital infrastructure being developed, which will increase material processing capability in space by two orders of magnitude. Indeed, past experience shows that the lifetime of advanced technologies is relatively short and that the need for new materials rapidly evolves. This had been illustrated in this report with the ICF project where a border-line silica-calcia glass used as a laser host was superseded by a fluorophosphate glass for its lower non-linear refractive index within a few years. Finally, it must not be forgotten that long-term R & D often benefits from unexpected results and that innovation frequently proceeds from fortuitous associations of emerging techniques.

Thus, the impact of GPS on industry in the long range cannot be appreciated on a specific basis since it relates to needs years ahead and therefore generally ill-defined. This is why it is unwary to make predictions on the industrial impact of GPS on the basis of the simple and irrelevant extrapolations of present needs.

Consequently, for the time being the development of GPS should rather be appreciated over a short-range period which expands up to the setting in operation of the permanent space infrastructure. This period will still be characterized by few flight opportunities and severe limitations in instrumentation performance. It is therefore reasonable to anticipate that GPS activities during

this period may fall in items of the type of the five ones selected in the above, priorities being given to basic research on the one hand and to specific problems attached to space processing on the other hand. As far as materials of industrial interest are concerned, priority should be given to those materials which are involved in long-lasting, well-established and major programmes of the type supported by NASA (11, 12, 13) simply because i) they guarantee the continuity at a time when flight opportunities are limited and ii) they provide in general the basic background indispensable to conduct efficient GPS experiment.

LIST OF REFERENCES

1. *R.A. Happe,*
   J. Non-Cryst. Solids 3 (1970) 375-392

2. *G.F. Neilson & M.C. Weinberg,*
   23 (1977) 43-58

3. *M.C. Weinberg*
   The glass industry, march 1978, 22-27

4. *J. Zarzycki, G.M. Frischat, D.M. Herlach*
   Fluid Sciences and Materials in Space : European perspective.
   ed. H.U. Walter (Springer-Verlag 1987) 599-634.

5. *R.P. Chanay & E.G. Osburn,* Space processing applications rocket project, NASA technical memorandum 82578.

6. *W.R. Wilcox, R.S. Subramanian , M. Meyyappan, H.D. Smith, D.M. Mattox & D.P. Partlow,*
   Final contrat, NAS8-33017.

7. *C. Potard & P. Dussere*
   Adv. Space Res. 4 (1984) 105-108.

8. Government Industrial Research Institute (GIRI), Japan, 1988
   Private Communication.

9. CGE Research Center
   Final Report CNES n° 87/1297 (France)

10. *B.M. Hitch*
Mutations microgravity, ISSN 0983-2793, 2-(3) 15 mai 1988.

11. *D.C. Larsen & M.A. Ali*
IITRI Project n° D6096, final report
Space processing of chalcogenide glass,
NAS-8-30627, March 30, 1977

12. *R.L. Downs, M.A. Ebner & R.L. Nolen*, final report,
Glass shell manufacturing in space, NAS8-33103, Dec. 21, 1981.

13. *M.C. Weinberg, G.F. Neilson & M.A. Zak*, final report
A feasibility study of the production of low loss IR fibers in space
NAS7-918, Nov. 15, 1983.

VI. PREREQUISITES FOR AN EFFICIENT EXPLOITATION OF GPS

Opportunities of experiments in space are bound to be limited probably until the setting in operation of the permanent space infrastructure being developed. Therefore, it is necessary to take all provisions in order to guarantee the relevance of the experiment, to insure a good functionning of the instrumentation and to be able to fully exploit the results. These conditions imply a solid basic and experimental background in the field under investigation, the development of a reliable and sophisticated instrumentation specifically dedicated to the needs and a multidisciplinary team able to exploit all the aspects of the experiment.

A direct consequence of this reasoning is that priority should be given to those GPS experiments which can take advantage of both solid experimental and theoretical basis, as this was the case for some American programmes cited in the above. This statement does not mean that "gedanken" experiments are prohibited but simply that a priority should be established among candidate experiments in order to allow a maximal chance of success. As far as glasses of industrial interest are concerned, this would restrict the choice to those materials involved in major, long-lasting projects.

So far, GPS has suffered of considerable problems which primarily related to precipitate programming of immature experiments and instrumentation repeated failures. This past experience clearly suggests - at it does virtually for all MPS activities - that there are qualitative steps for a rational exploitation of the microgravity environment. In a next step, it will be essential to conceive simple experiments with clear and limited objectives using well-established materials. Basic investigations of the type conducted by G.H. Frichat and co-workers pertain to this category and are actually needed for the quantitative assessment of glass transformation kinetics. Furthermore, they fall in a category which may be well-suited for the use of multipurpose instrumentation. Experiments on thermomigration, glass fining, etc... are probably to be classified in the same

category.

The situation may be completely different with more sophisticated investigations relating e.g., to the search of vitrification domains of complex compound materials or to the preparation of reference glass samples for the evaluation of intrinsic properties. It is obvious that previous, extended ground-based studies are an absolute prerequisite in these cases simply because most often the nature of the crystallizing species, the pertinent parameters of transformation kinetics, the relevant thermodynamical data, not to mention processing conditions in space are unknown. Without the necessary knowledge such experiments are extremely hazardous. Therefore, all means should be deployed prior to any space experiment including basic research on the ground and whenever possible if relevant, short-duration free fall tests. Levitation tests on the ground performed by several laboratories on low-loss glasses and aimed at suppressing heterogeneous nucleation due to container walls, as does weightlessness, participate of this approach.

One must realize however that a dedicated instrumentation will generally be necessary for more complex experiments. The examples below illustrate this appreciation for the case of the preparation of reference samples. Some intrinsic properties, e.g., optical properties such as refractive indices, require samples $1cm^3$ in size which may be prepared with current acoustic positioning equipments. On the contrary, other properties such as the attenuation level will require large and shaped samples for evaluation purposes and extremely well-controlled temperature profiles during cooling in order to prevent scattering due to density fluctuations. For these experiments, multipurpose experiments are certainly prohibited and new positioning concepts, e.g. gas film levitation, may have to be developed.

CONCLUSIONS

Despite its long history, glass technology generally suffers from insufficient basic background, especially in the case of complex compound systems where the crystallizing species are seldom identified and the pertinent thermodynamical data which relate to glass transformation kinetics are not known. This makes theoretical evaluations of transformation kinetics and predictions on vitrification domains illusory for most systems of interest to industry.

In the future, this situation may rapidly evolve because of the increasing demand of advanced technology in glasses for their ability to be tailored at will - as opposed to crystalline materials - by the use of their enormous compositional potential. Candidate glass families are relatively keen to vitrify and therefore extremely sensitive to heterogeneous nucleation.

In this context, glass processing in space (GPS) offers unique possibilities mainly by allowing containerless processing. It is true that to-day the potential of GPS has hardly been unveiled because of a laborious learning period hindered by a lack of flight opportunities. Nevertheless, GPS may rapidly turn out to be at the cross-roads of the most advanced studies in the glass area, if properly exploited. Preliminary cross-fertilization between 1-g and 0-g experiments already supports this point of view.

For the time being, it is difficult if not impossible to make safe predictions on the impact of GPS on glass industry. It is highly probable that GPS activities will stay at a modest level until the setting in operation of permanent orbital infrastructures because of a lack of flight opportunities. In the meantime, it may be advantageous to establish a priority among the space experiments to be conducted and to develop dedicated instrumentations.

Priorities may be given to studies on systems, which already benefit from a strong, multidisciplinary scientific background, in the following directions : acquisition of basic data, preparation of reference samples and investigations on space-adapted processes. Such studies could be completed by vigorous programmes on the ground in order to make the exploitation of space experiments less hazardous that it has been in the past.